THESIS

ATMOSPHERIC REACTIVE NITROGEN IN ROCKY MOUNTAIN NATIONAL PARK

Submitted by

Yixing Shao

Department of Atmospheric Science

In partial fulfillment of requirements

For the Degree of Master of Science

Colorado State University

Fort Collins, Colorado

Spring 2018

Master's committee:

Advisor: Jeffrey L. Collett Jr.

Russ Schumacher
Shantanu Jathar
Katherine Benedict

ABSTRACT

ATMOSPHERIC REACTIVE NITROGEN IN ROCKY MOUNTAIN NATIONAL PARK

The Front Range urban corridor in Colorado, located east of Rocky Mountain National Park (RMNP), includes a variety of urban sources of nitrogen oxides, while high emissions of ammonia are found in agricultural sources on the eastern plains of Colorado. The spatial distribution and temporal variation of ammonia and other reactive nitrogen species in the region is not well characterized. Periods of upslope flow can transport atmospheric reactive nitrogen from the Front Range and eastern Colorado, contributing to nitrogen deposition in the park. Deposition of excess atmospheric reactive nitrogen in Rocky Mountain National Park poses threats to sensitive ecosystems. It is important to characterize temporal variation and spatial distribution of reactive nitrogen in the region to better understand the degree to which emission sources in the northeastern plains of Colorado impact RMNP and how meteorological conditions are associated with transport of ammonia to the park.

Mobile and in-situ measurements of reactive nitrogen gases and particles were made between 2015 and 2016 in northeastern Colorado and RMNP. Gaseous ammonia was measured with high-time resolution instruments (a Picarro cavity-ring down spectrometer and an Air Sentry ion mobility analyzer); 24-hr integrated concentrations of trace gases and $PM_{2.5}$ chemical composition in RMNP were measured by URG denuder/filter systems coupled with lab analysis; wet nitrogen deposition was collected with an automated precipitation collector followed by lab analysis. Model outputs from The Hybrid Single Particle Lagrangian Integrated Trajectory Model (HYSPLIT) was also included for examining transport of ammonia source plumes.

Diurnal and seasonal variability of ammonia concentrations and some other reactive nitrogen species were characterized with high time-resolution measurement data. Repeating diurnal cycles were found in Greeley and RMNP. Ammonia concentrations usually increase in the morning and reach maxima around noon in RMNP, while at Greeley ammonia builds up during the night followed by a rapid decrease after sunrise. A seasonal pattern of ammonia levels was also revealed, with higher concentrations observed during summer. When combined with wind data it is clear that elevated ammonia levels in RMNP were associated with easterly transport from the eastern plains of Colorado. The median daily averaged ammonia concentrations measured in Greeley, Loveland and RMNP are 26.2 ppb, 6.3 ppb and 0.97 ppb respectively. Considerable ammonia variability was found in NE Colorado with higher concentrations measured close to CAFOs and source regions. This was particularly clear in mobile NH_3 observations where distinct plumes of ammonia were observed away from confined animal feeding operation (CAFOs) sources. Spatial variations, particularly in the north-south direction, were observed to be strongly dependent on meteorology as highlighted by HYSPLIT back trajectories.

This study also evaluates the pilot Early Warning System which informs agricultural producers of impending upslope events that are likely to transport nitrogen from eastern Colorado to the park, so that management practices may be implemented to reduce nitrogen emissions. The performance of the meteorological forecasting was evaluated using continuous measurements of atmospheric ammonia concentrations in the RMNP, as well as the wet nitrogen deposition data from 2015. It was found that the model showed skill in capturing some large wet nitrogen deposition events in the park.

ACKNOWLEDGEMENTS

The project was supervised and directed by Professor Jeffrey L. Collett Jr., with support and funding from the National Park Service and Colorado Department of Public Health and Environment. I would like to acknowledge Professor Jeffrey L. Collett Jr. for his contribution of time, ideas and guidance for this project, as well as providing exciting research opportunities for me. I am also grateful to my other committee members, Professor Russ Schumacher, Professor Shantanu Jathar and Dr. Katherine Benedict for their insightful comments and recommendations for this work. A very special acknowledgement goes to Dr. Katherine Benedict for her guidance and support throughout the study.

Special recognition goes to people who have helped with the field measurements. The in-situ field measurements were conducted with significant contributions from Katherine Benedict, Amy Sullivan, Ashley Evanoski-Cole and Evie Bangs; the mobile measurements were conducted with coordination from Arsineh Hecobian. I also would like to thank all other past and present members of the Collett group for fulfilling my experience in Colorado State University academically and personally.

I also thank my husband, family and friends for support and encouragement.

TABLE OF CONTENTS

LIST OF TABLES

LIST OF FIGURES

CHAPTER 1 - INTRODUCTION

1.1 Reactive Nitrogen in the Atmosphere

Reactive nitrogen in the atmosphere generally refers to all photochemically, biologically and radiatively active nitrogen compounds within the Earth's atmosphere, both in the gaseous phase and particulate phase (Sobota et al., 2013). Relatively unreactive nitrogen gas (N_2) contributes more than 99.99% of nitrogen present in the atmosphere, with other nitrogen compounds present at trace levels (Wallace and Hobbs, 2006). Reactive nitrogen species are often classified as inorganic or organic forms, and as reduced or oxidized. In general, oxidized inorganic nitrogen species include HNO_3, NO_3^-, and NO_x, whereas ammonia (NH_3) and ammonium (NH_4^+) are referred as reduced inorganic nitrogen compounds. Other important reactive organic nitrogen species in the atmosphere include peroxyacetyl nitrate (PAN), amines and alkyl nitrates.

With the rapid growth of Earth's population after the discovery of the Haber-Bosch process that allows efficient nitrogen fertilizer production for increased food supply, the global nitrogen cycle has been largely influenced with further impacts on the nitrogen cascade in the environment (Galloway and Cowling, 2002, Galloway et al., 1995). The presence of human activities has strongly altered the global biogeochemical nitrogen cycle; increased reactive nitrogen in the atmosphere contributes to formation of particulate matter and tropospheric ozone (Chameides et al., 1992; Andreae et al., 1997; Fowler et al., 1998; Park et al., 2004; Sutton et al., 2011), ozone depletion in the stratosphere (Ravishankara et al., 2009), climate change (Erisman et al., 2011; Pinder et al., 2012). Excess reactive nitrogen in the atmosphere may also pose threats to sensitive terrestrial and aquatic ecosystems (Rabalais et al., 2002; Gruber and

Galloway, 2008;) and impact human health and welfare (Vitousek et al., 1997; Wolfe et al., 2002; Townsend et al, 2003).

1.1.1 Reduced Inorganic Nitrogen (NH_3)

Ammonia is the most abundant basic gas in the atmosphere and can serve as a neutralizer for ambient acids, such as nitric acid (HNO_3) and sulfuric acid (H_2SO_4). The main sources of ammonia emissions are from agricultural activities in many regions of the world, including animal husbandry or fertilizer application. The 2011 National Emission Inventory (https://www.epa.gov/air-emissions-inventories/2011-national-emissions-inventory-nei-data) provides an estimate of ammonia emissions from various sources, indicating that approximately 83.90% of the total anthropogenic ammonia emissions in the US are from agricultural sources. Other important sources for ammonia emissions include on-road engines and vehicles (Kean et al., 2000; Kean et al., 2009) present as 2.53% of the total, and biomass burning (Hegg et al., 1988) present as 10.55% of the total anthropogenic ammonia emissions in the 2011 National Emission Inventory. Ammonia in the atmosphere has a lifetime of a few hours with respect to deposition, while ammonium and nitrate in the particle phase usually has longer lifetime (a few days) and can be transported for longer distances.

Ammonia can be measured both in-situ or from space. In-situ measurements of ammonia are generally conducted by one of three approaches: 1) Passive devices that provide integrated values of ammonia captured by diffusion during a period of time; 2) Integrated methods (denuders) that provide measurements of ammonia by drawing air through a denuder or filter and capture on a coated surface; 3) Continuous instruments, including cavity ring-down, ion mobility, and wet chemistry instruments, that sample at higher frequency and provide near real-

time measurements of ammonia/amines. In addition, instruments on board satellites have been deployed in measuring ammonia and other trace gases from space. Such instruments include the Tropospheric Emission Spectrometer/Aura (TES), Infrared Atmospheric Sounding Interferometer/Metop (IASI), Cross-track Infrared Sounder/NPP (CrIS) and Atmospheric Infrared Sounder/Aqua (AIRS). Satellites provide measurements of ammonia concentrations integrated across some range of altitudes and generally offer measurements that are more representative than a single ground-based measurement for a broad area (Van Damme et al., 2015). Since these satellites are orbiting around the earth, measurement over a particular location is not continuous temporally.

1.1.2 Oxidized Inorganic Nitrogen (NO_x and HNO_3)

NO_x is produced from combustion processes as a result of reactions between nitrogen and oxygen gases. Based on the EPA 2011 National Emission Inventory Data, on-road vehicles represent 37.78% of total national NO_x emission while electric utilities account for 13.45% of the total. Another important source for NO_x emission is industrial fuel combustion (8.10%).

Nitric acid is formed in the atmosphere through oxidation of NO_x ($NO + NO_2$) during the daytime according to (Eqn. 1.1).

$$NO_2 + OH \rightarrow HNO_3 \quad \text{(Eqn. 1.1)}$$

Lacking photochemical activity during the night; the primary overnight source for HNO_3 is through the hydrolysis reactions of dinitrogen pentoxide (N_2O_5) and NO_2 (Eqn. 1.2-1.3).

$$N_2O_5 + H_2O \rightarrow 2HNO_3 \quad \text{(Eqn. 1.2)}$$

$$2NO_2 + H_2O \rightarrow HNO_2 + HNO_3 \quad \text{(Eqn. 1.3)}$$

Other reactions that lead to production of HNO_3 in the atmosphere include reaction with nitrate radicals (Eqn. 1.4-1.5): (Seinfeld and Pandis, 2012)

$NO_3 + H_2O \rightarrow HNO_3$ (Eqn. 1.4)

$NO_3 + HONO \rightarrow HNO_3 + NO_2$ (Eqn. 1.5)

Nitric acid has an atmospheric lifetime of hours up to a few days and efficient pathways for its removal from the atmosphere are through precipitation washout and surface dry deposition. HNO_3 is one of the most important acidic gases in the atmosphere and contributes to particle formation. It reacts with alkaline species in the atmosphere to form particulate nitrate.

HNO_3 can be measured by passive samplers, filters, denuders and continuous instruments. Various satellite products also retrieve information of tropospheric HNO_3 concentrations, such as the Tropospheric Emission Spectrometer/Aura (TES), Infrared Atmospheric Sounding Interferometer (IASI) /MetOp, High Resolution Dynamics Limb Sounder (HIRDLS)/Aura.

Particulate nitrogen ammonia in the atmosphere can react with acidic constituents to form particulate nitrogen species, such as ammonium nitrate (Eqn 1.6), ammonium bisulfate (Eqn 1.7) and ammonium sulfate (Eqn 1.8).

$HNO_3 + NH_3 \leftrightarrow NH_4NO_3$ (Eqn. 1.6)

$H_2SO_4 + NH_3 \rightarrow NH_4HSO_4$ (Eqn. 1.7)

$NH_4HSO_4 + NH_3 \rightarrow (NH_4)_2SO_4$ (Eqn. 1.8)

Sulfuric acid and ammonium bisulfate will take up ammonia from the gas phase when it is available, regardless of ambient conditions. The gas-particle partitioning of ammonium nitrate, by contrast, is quite sensitive to temperature and humidity. Ammonia and nitric acid tend to

remain in the gas phase, rather than form ammonium nitrate, under high ambient temperature and low relative humidity (Stelson and Seinfeld, 1982).

1.1.3 Organic Nitrogen

Organic compounds that contain both carbon and nitrogen may be referred to as organic nitrogen. Organic nitrogen in atmosphere presents in various form, including gas, particles and dissolved phases, with large spatial and temporal variability (Cape et al., 2011). Amines are derivatives of ammonia and have acid-neutralizing capacity in formation of particles. Important sources for amines include animal wastes, combustion processes and sewage (Ge et al., 2010). Other important reactive organic nitrogen species in the atmosphere include amino acids, urea, peroxyacetyl nitrate (PAN), alkyl nitrates.

1.2 Nitrogen Deposition

1.2.1 Deposition Processes

Nitrogen deposition is defined as atmospheric reactive nitrogen species being deposited to the surface of the earth either through wet or dry deposition processes. Dry nitrogen deposition refers to the deposition of nitrogen-containing compounds (gases and particles) to the Earth's surface without involvement of atmospheric hydrometeors. Reactive nitrogen species can be dry deposited to the surface of the Earth via processes including diffusion, impaction, interception, and gravitational sedimentation (Seinfeld and Pandis, 2012). HNO_3 and particles are irreversibly deposited to surfaces. Ammonia doesn't behave the same way; bi-directional exchange between the atmosphere and surface means that ammonia deposited, for example to plants, can be re-

emitted to the atmosphere. Vegetation, soils, and litter, can serve as both sources and sinks for atmospheric NH_3 (Sutton et al., 1995).

Wet nitrogen deposition refers to deposition of reactive nitrogen gases and particles from the atmosphere to the Earth's surface by precipitation (Seinfeld and Pandis, 2012). In-cloud scavenging is when particles or gases are captured by cloud drops and then transferred to precipitation (rain drops or snow crystals) inside the cloud. This process determines the initial concentrations of trace species inside the precipitation falling out of the cloud. Below-cloud scavenging refers to the capture of reactive nitrogen particles and soluble gases that are below clouds by rain or snow and subsequent deposition to the surface. The efficiency of in-cloud and below-cloud wet deposition processes depend on various microphysical characteristics of the cloud, solubility/hygroscopicity of gases/particles, and collision/scavenging efficiency.

Other less understood processes can remove nitrogen species from the atmosphere either temporarily or permanently depending on chemistry and environmental factors. An example of this is the interactions of dew droplets with boundary layer NH_3. The work of Wentworth et al. (2016) shows that NH_3 can be taken up by dew as it forms overnight and then re-emitted to the atmosphere in an early morning pulse of ammonia as the dew evaporates. It is possible that nitric acid could be involved in a similar process but may not be as efficiently re-emitted to the atmosphere, especially if NH_3 is in large excess.

1.2.2 Negative Effects of Excess Nitrogen Deposition

Excess nitrogen deposition to the surface of the earth may impact terrestrial ecosystems, aquatic ecosystems and biodiversity (Vitousek et al., 1997; Lee et al., 1998; Sala et al., 2000; Matson et al., 2002; Phoenix et al., 2006; Galloway et al., 2008). Research by Baron et al. (1994)

examined the nitrogen saturation potential of the vegetation in RMNP, indicating that high nitrogen loads were produced in aquatic ecosystems in the park. Wolfe et al. (2000) used nitrogen isotopes to study anthropogenic nitrogen deposition in the alpine lakes in Colorado Front Range area, and found that nitrogen deposition has resulted in limnological changes in the pristine areas and such change has exceeded the natural variability. A study using sediment cores in RMNP has shown that alpine lakes in the park are impacted by anthropogenic nitrogen deposition by altering diatom community composition (Wolfe et al., 2003). The forest and soil chemistry in RMNP is also subject to change due to excess nitrogen deposition (Baron et al., 2000). Efforts have been devoted in determining N loads for vegetation and alpine lakes in RMNP, and observed nitrogen deposition of 3 kg N ha^{-1}\ yr^{-1}, exceeding critical loads, has resulted in decreasing plant diversity and changes in aquatic systems in the park (Baron, 2006; Bowman et al., 2012).

A lab/field study by van den Berg et al. (2016) found that ecosystems react differently to reduced versus oxidized nitrogen deposition. They determined that biodiversity of grasslands is negatively or positively impacted by nitrogen deposition, depending on the form of nitrogen deposited. With management strategies focused on reducing NO_x emissions, there has been evidence showing wet deposition of reduced nitrogen has become increasingly important in the United States while oxidized nitrogen deposition has shown significant decreases over recent decades (Li et al., 2016). This trend, combined with different ecological responses for oxidized and reduced nitrogen, is an important consideration for future patterns of deposition and ecological response.

1.2.3 Previous Nitrogen-Related Studies in Colorado

Based on observed impacts of excess reactive nitrogen deposition, a 2007 memorandum of understanding (MOU) was signed by the National Park Service (NPS), the U.S. Environmental Protection Agency (EPA), and the Colorado Department of Public Health and Environment (CDPHE) to increase efforts to reduce nitrogen deposition in RMNP (NPS, EPA, CDPHE 2007). This Rocky Mountain Nitrogen Reduction Plan (RMNRP) (http://www.colorado.gov/cdphe/rmnpinitiative) proposed a "glidepath" designed to reduce wet nitrogen deposition received by RMNP to a critical load value (1.5 kg/ha/yr) by 2032.

A few national networks have long-term documentation of air quality and wet deposition in Rocky Mountain National Park, including two National Acid Deposition Program/National Trends Network (NADP/NTN) sites as well as Interagency Monitoring of Protected Visual Environments (IMPROVE) and Clean Air Status and Trends Network (CASTNet) sites. Several field campaigns were conducted in RMNP and northeastern Colorado in recent years to study air quality and deposition fluxes (Baron, 2006; Baron et al, 2000; Burns, 2003; Day et al, 2012; Beem et al, 2013a,c). Other mobile measurements were conducted to examine ammonia emissions from various sources, such as on-road vehicles and animal husbandry (Sun et al, 2014; Miller et al, 2015; Tao et al, 2015). Modeling systems have been utilized for source apportionment of the reactive nitrogen species that contribute to total nitrogen deposition in RMNP (Gebhart et al, 2011; Gebhart et al, 2014; Malm et al, 2013; Thompson et al, 2015). Measurements of atmospheric reactive nitrogen concentrations and deposition provide long-term records for trends study, while modeling work provides useful context and background in nitrogen-related research and aids scenario testing and decision making.

The following chapter details the methods used for field measurements and data acquisition. The instrument calibration methods and quality assurance in addition to data analysis is also provided. In the result chapter, measurements of various gaseous and particulate reactive nitrogen species in northeastern Colorado and Rocky Mountain National Park were presented, both in situ and on board a mobile vehicle. Collocated measurement of ammonia gas with different measurement techniques, including URG denuder/filter system, Picarro Cavity Ring-Down Spectroscopy and Air Sentry Ion Mobility Spectrometer, will be analyzed and compared. Temporal variability and spatial distribution of ammonia and some other reactive nitrogen species will be examined and characterized with measurement taken in the NE Colorado and RMNP. Transport of ammonia from the northeastern plains of Colorado to the park will be investigated using measurement data and a Hybrid Single Particle Lagrangian Integrated Trajectory Model. In addition, the performance of the pilot Early Warning System aiming in reducing nitrogen deposition will be evaluated with wet deposition measurements and gas/particle concentrations, in terms of its ability in tracking the air parcel endpoints and forecasting the high wet deposition periods. Conclusions are included in Chapter 4 and future work is included in Chapter 5.

CHAPTER 2 - EXPERIMENTAL METHODS

2.1 Sampling Sites

The northeastern plains of Colorado provide a valuable and unique case in studying spatial distribution and transport of reactive nitrogen. The Front Range urban corridor in Colorado consists of a variety of urban sources for oxidized nitrogen, while high emissions of reduced nitrogen are found in agricultural sources on the eastern plains of Colorado (Gebhart et al., 2011; Malm et al., 2009). Data from the National Emission Inventory (NEI) reveal that ammonia emissions are higher in the northeastern part of Colorado, including Weld, Logan, and Morgan counties (Figure 2.1.1).

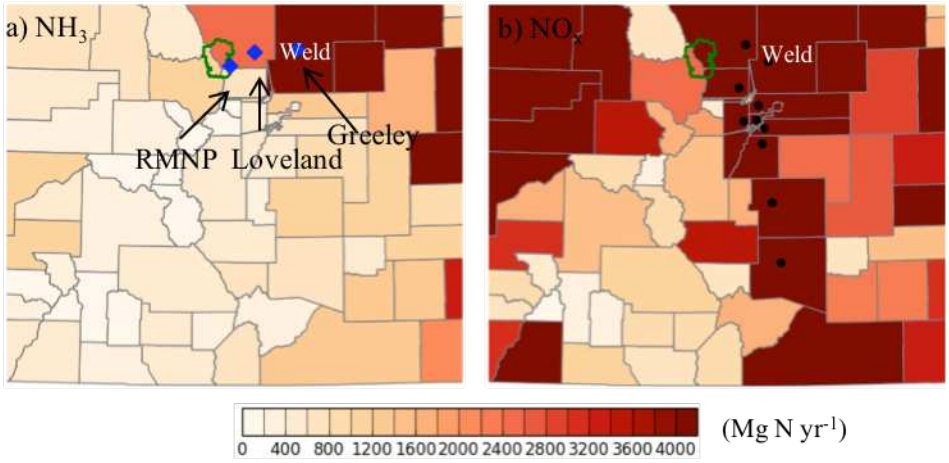

Figure 2.1.1 2011 National Emission Inventory of a) NH_3 (Mg N yr^{-1}) and b) NO_x (Mg N yr^{-1}) by county in Colorado. Blue diamonds in a) indicate sites for continuous NH_3 measurements in RMNP, Loveland and Greeley. Black dots in b) show population centers with more than 150,000 residents. RMNP is outlined in green.

The 2011 NEI for ammonia includes emissions from agricultural operations, industrial processes, fuel combustion, on-road vehicles and fires. The annual totals of 53,807 tons and 15,087 tons of NH_3 emissions are from livestock waste and fertilizer application respectively,

which account for 68% and 19% of total ammonia emissions. The 2011 NEI shows that 87% percent of NH_3 emissions in Colorado are from agricultural sources. High emissions of NO_x in NE Colorado are found in the Front Range urban corridor, where most of the urban population is located. Weld County, sitting less than 100 miles east of RMNP, is a leading agricultural producing county in Colorado. It has the highest emissions of ammonia and NO_x among all counties in Colorado, with annual NH_3 and NO_x emission of 16,091 Mg N and 32,696 Mg N respectively.

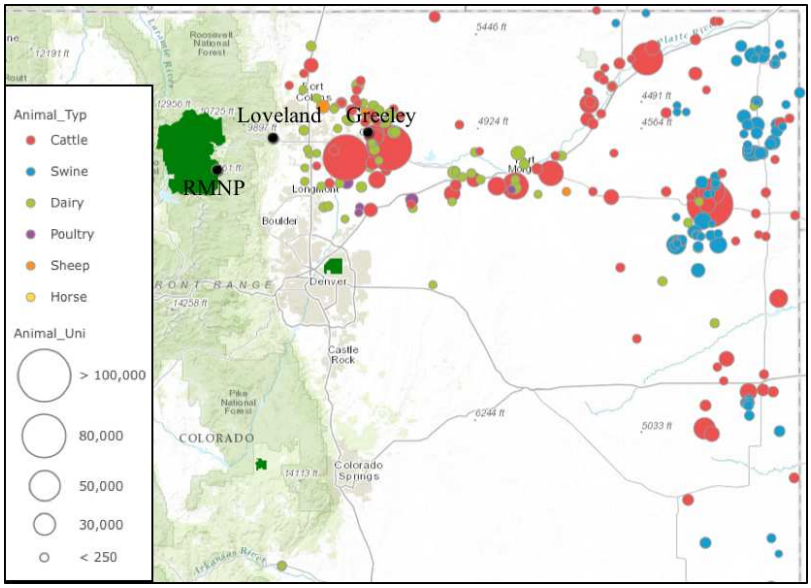

Figure 2.1.2 Map of northeastern Colorado with locations and sizes of Confined Animal Feeding Operations (CAFOs). The dot sizes indicate animal units; animal types are colored with red for cattle, blue for swine, green for dairy, purple for poultry, orange for sheep and yellow for horses. Black dots indicate air quality monitoring sites in RMNP, Loveland and Greeley. Rocky Mountain National Park is shaded in green.

Confined animal feeding operations (CAFOs) are shown as the maximum permitted capacity of animal units, which is a type of animal counting that is different than the headcounts (data are from the Colorado Department of Public Health and Environment). U.S. Environmental Protection Agency (EPA) defines an animal unit as an animal equivalent of 1000 pounds live

weight and equates to 1,000 head of beef cattle, 700 dairy cows, 2,500 swine weighing more than 55 lbs, 125,000 broiler chickens or 82,000 laying hens or pullet. (https://www3.epa.gov/npdes/pubs/cafo_permitmanual_chapter2.pdf). A CAFO is an animal feeding operation with more than 1000 animal units confined on site for more than 45 days during the year. (https://www.nrcs.usda.gov/wps/portal/nrcs/main/national/plantsanimals/livestock/afo/)

Three air quality monitoring sites were used to collect data for this study. The site in RMNP (40.2782, -105.5460) is located 3 miles south of Lily Lake and is at the foot of Long's Peak with elevation of 2760 m above mean sea level. This site is also home to monitoring activities for the IMPROVE (Interagency Monitoring of Protected Visual Environments) and CASTNET (Clean Air Status and Trends Network) programs. The site in Greeley, CO (40.3863, -104.7374) is in an area with extensive CAFOs, including beef cattle, dairy cows, poultry, swine, sheep and horse, which are large sources of ammonia and methane emissions (Eilerman et al., 2016). Ammonia emissions from the Greeley region have been shown to strongly influence the concentrations and deposition of ammonia in Rocky Mountain National Park (Malm et al., 2013). The biggest cattle CAFO (125150 animal units) of Weld County is located less than 10 miles southeast of the Greeley site. Other smaller CAFOs, mainly cattle and dairy feedlots, surround the Greeley site. The Loveland site (40.4239, -105.2115) is located near the Loveland Water Treatment Plant, very close to the foothills of the Rocky Mountains.

Collocated meteorological data is available with a time resolution of 1 hour in RMNP, while Greeley and Loveland have 5-minute data available for portions of the measuring periods. Temperature and wind information for the Greeley site were obtained from the Colorado Department of Public Health and Environment (CDPHE). Collocated meteorological data at the

RMNP Long's Peak (ROM406) site, including temperature, wind direction and speed, precipitation, were obtained from the CASTNET program.

Table 2.1.1 Timetable of various measurement techniques and time resolution in Greeley, Loveland and RMNP sites used in the thesis.

Sites	Year	URG denuder/filter	Air Sentry IMS	Picarro CRDS	Wet Deposition
RMNP	2014	07/07-10/14	07/12-09/08 (5 sec)		07/07-10/10
	2015	03/14-10/15		03/13-10/25 (1 min)	03/18-10/07
	2016	03/14-10/19	03/11-10/28 (5 sec)	08/10-10/28 (1 min)	03/14-10/17
Loveland	2015		07/22-10/26 (5 sec)		
	2016		03/11-10/15 (5 sec)		
Greeley	2015		03/16-10/27 (5 sec)		
	2016		08/11-10/18 (5 sec)	04/15-10/01 (1 min)	

The three monitoring sites were chosen to help to characterize the spatial distribution of ammonia, especially the west to east gradient, in NE Colorado. Continuous high time-resolution ammonia observations began in 2014 and continued through 2016 from spring to fall (see Table 2.1.1 for exact measurement dates). Two different instruments were used for measuring real-time ammonia concentrations, a Picarro cavity ring-down spectroscopy analyzer (G2103) and a Particle Measurement Systems Air Sentry II ion mobility spectrometer. Wet deposition was also measured at the RMNP site. URG denuder/filter trains were used to measure daily trace gases and $PM_{2.5}$ chemical composition in RMNP.

2.2 Sampling Techniques

2.2.1 URG Annular Denuder/Filter-Pack System

The URG annular denuder/filter-pack system (URG-3000CA) is a manual sampling system that collects both acidic and basic gases and particles (Figure 2.2.1). This technique has been widely adopted in studies for aerosol and trace gas measurements (Edgerton et al, 2007; Lee et al., 2008a; Lee et al., 2008b; Beem et al., 2010; Puchalski et al., 2011; Tsai et al., 2013). The URG denuder/filter-pack sample trains were installed at 1.5m above ground in an insulated sampling box. Ambient air was drawn through the sample train by a pump at a regulated flow rate of 10 L min^{-1} at RMNP. A dry gas meter is connected to the system to measure the total volume of air sampled. The sample train is set up as follows. First, a Teflon coated cyclone removes all the coarse particles that have an aerodynamic diameter greater than 2.5μm. Air then passes through a denuder coated with sodium carbonate to trap acidic gases, such as nitric acid and sulfur dioxide, and then a second denuder coated with phosphorous acid collects gaseous ammonia. Air is then drawn through a filter-pack loaded with a 47mm diameter nylon filter that has pore size of 1μm (Nylasorb, Pall Corporation).

The filter retains particulate matter, including Na^+, K^+, Mg^{2+}, Ca^{2+}, Cl^-, SO_4^{2-}. NH_4NO_3 particles are semivolatile and their volatilization can introduce a filter sampling bias. A previous study (Yu et al., 2006) reviewed the performance of a denuded nylon filter sampling system under a wide variety of conditions and confirmed NO_3^- is not lost from the nylon filter. While the nylon filter is efficient at retaining volatilized nitric acid, volatilized NH_4^+ particles are not well retained by the filter and thus a backup denuder, coated with the same phosphorous acid solution, is installed after the filter-pack to capture any volatilized ammonium, typically due to changes in temperature and relative humidity during the sampling period. The total particulate ammonium

concentration is calculated by adding ammonium/ammonia collected from the backup denuder and filter together.

All the sample trains are prepared in the lab of Colorado State University (CSU), and then kept in a refrigerator before being brought to the field site. Measurements with URG denuder/filter are taken daily in RMNP from 09:00 am to 09:00 am (next day) and weekly (starting every Tuesday) at Greeley. Blank denuder and filter trains were installed every Monday at RMNP site, and then taken back to the lab on Wednesday. The denuders are extracted with 10 ml deionized water, and the extracts are kept refrigerated before analysis. Nylon filters are extracted with 6 ml deionized water in an ultrasonic water bath for an hour, and then stored in a refrigerator until ion chromatography analysis.

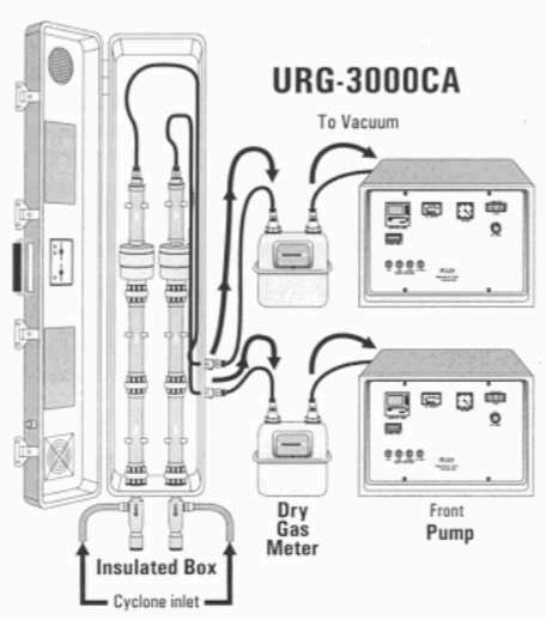

Figure 2.2.1 A schematic diagram of dual channel URG denuder/filter sampling system (URG Inc product catalog).

Extra denuder/filter trains were deployed to the RMNP site to collect samples where the position of the ammonia and nitric acid denuders were reversed. The comparison of ammonia gas concentrations measured by the two installations is shown as Figure 2.2.2 a) with a least

square fit applied (y=0.83x-0.03, R^2 =0.95). There is a low bias in the collection of ammonia when the ammonia denuder is in the second position. This might be due to the "sticky" characteristic of ammonia which tends to interact with surfaces and results in losses of ammonia. Based on the trend line fitted to these 7 replicates in measuring ammonia concentrations, 17% less ammonia can be captured when denuder trains are installed with the HNO_3 denuder in the first position.

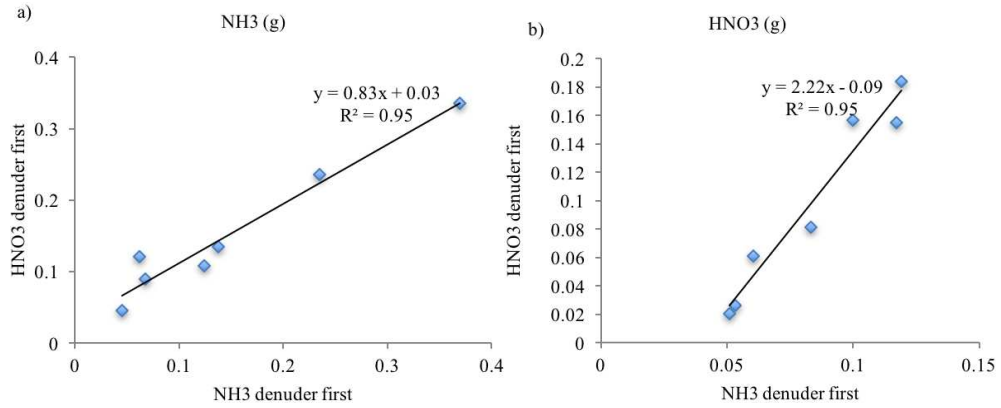

Figure 2.2.2 Comparison of gaseous a) ammonia and b) nitric acid concentrations (g) measured by denuders with the NH_3 denuder first and the HNO_3 denuder first.

The same comparison was done for nitric acid gas, which is also a "sticky" gas. It is found that the least square fitting line is y=2.22x-0.09 with R^2 =0.95 when comparing gaseous nitric acid measured by NH_3-absorbing being first position to the one with HNO_3-absorbing denuder being the first. The slope being 2.22 indicates that the amount of the HNO_3 gas captured by normal-order denuder trains is more than twice the result given by the reversed-order denuder trains. This is why the HNO_3 denuder is normally operated in the upstream position.

2.2.2 Wet Nitrogen Deposition Chemistry

An automated total precipitation collector is used to acquire precipitation samples for which wet nitrogen deposition is analyzed. The precipitation sampler (Yankee Environmental

System Inc.) opens a lid automatically when precipitation is detected. Precipitation is collected in a clean bucket prepared in the CSU lab and brought to the site. The bucket was rinsed with deionized water multiple times and covered with a piece of clean foil until installation in the sampler. Once precipitation ceases, the lid of the sampler closes automatically to avoid any contamination from ambient air and also to prevent precipitation from evaporating. The wet deposition bucket in RMNP was changed on Monday, Wednesday and Friday resulting in either 2 or 3 days integrated samples. The sample weight is measured at the site and then the collected sample is transferred to a clean bottle and brought back to CSU. All the samples were kept frozen until analysis by ion chromatography.

2.2.3 Picarro Cavity Ring-Down Spectroscopy

Cavity Ring-Down Spectroscopy (CRDS) technique provides ammonia measurements with high time-resolution and precision in the field (von Bobrutzki et al., 2010, Benedict et al., 2013b). The CRDS technique (Figure 2.2.3) makes use of the uniqueness of the near-infrared absorption spectrum of ammonia gas and measures the strength of its absorption. The Picarro CRDS analyzer (G2301) uses a three-mirror cavity, which allows the effective path length of absorption to be many kilometers, to increase the analyzer sensitivity for ammonia to parts-per-trillion (ppt) level (www.picarro.com/technology/cavity_ring_down_spectroscopy).

Figure 2.2.3 shows schematics for the Picarro CRDS analyzer. At the detector voltage build-up stage, the cavity quickly fills with laser light. When the laser is abruptly turned off, the light within the cavity bouncing between reflective mirrors and the light intensity decay in an exponential fashion (Wheeler et al., 1998; Paldus et al., 2005). This decay, also known as the "ring-down" process, is measured by a photodetector. When ammonia gas is introduced into the

cavity, ring-down time is accelerated due to absorption. The Picarro CRDS measures the ring-down time with and without the targeted gas species for speciation and quantification. The inlet Teflon-coated tubing was heated by a heating tape to 40°C to prevent condensation of water and to prevent ammonia from sticking to the inlet surface (Ellies et al., 2010). Samples were drawn through the same heated inlet tubing for measurement with the Picarro CRDS analyzer and other high time-resolution ammonia measurement instruments.

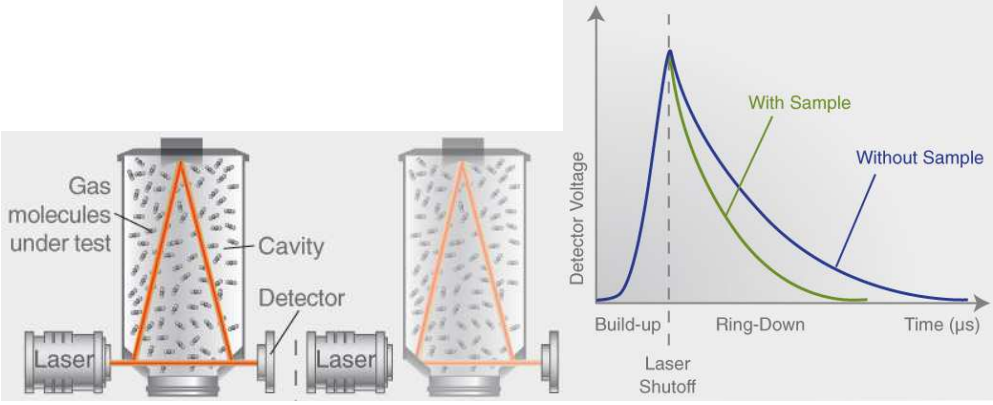

Figure 2.2.3 Schematics for the Picarro Cavity Ring-Down Spectroscopy Analyzer (www.picarro.com/assets/images/content/cavity_figure_large.jpg) and ring down measurements (www.picarro.com/assets/images/content/ring_down_large.jpg).

2.2.4 Air Sentry II Point-of-Use Ion Mobility Spectrometer

Ion Mobility is a measurement technique used to detect and identify ionized molecules based on their mobility in a carrier buffer gas. The AirSentry II Point-of-Use Ion Mobility Spectrometer (IMS, Particle Measuring Systems) provides high time-resolution measurements of ambient gaseous ammonia and amines within a range of 0-50 ppb, with manufacturer-specified part-per-trillion (ppt) sensitivity and fast response. This instrument has been used for ammonia measurements in pristine region (Grand Teton National Park) and showed good capability in low-concentration environments (Prenni et al., 2014). First, air sample was drawn through a heated Teflon tubing to reduce ammonia losses to the tubing. Then the sample gets ionized with

a radioactive ^{63}Ni β-emitter, and then enters a drift tube containing buffer gas. The ions move through the drift tube in the presence of an electric field and get detected on a collector plate, yielding a spectrum that can be interpreted by a software algorithm in real-time. The flight time of a target analyte inside the drift tube is a function of ion mobility and is used for speciation; detected peak height is used for quantification (Hill et al., 1990). The instrument needs to be "zeroed" when moved to a new sampling site to adjust for any differences in altitude (pressure) which alter the expected time-of-flight for the reagent and sample peaks. A Teledyne zero air system (model 701 at Loveland and Greeley and model 751 at RMNP) is used to provide ammonia-free air to the system, while gas cylinders are used on our mobile platform to provide clean dry air (CDA) to the Air Sentry system. The heated inlet tubing for the Air Sentry II ammonia monitor is the same as for the Picarro CRDS analyzer. Zero checks were done periodically throughout the measurement period, and a multi-point calibration was done at the end of the study.

2.2.5 Calibration of Picarro CRDS and Air Sentry IMS

Calibrations for the high time-resolution ammonia measurement instruments were done at the end of each measurement year, in the field when possible. Time-averaged measurements of ammonia taken by the Picarro CRDS and the Air Sentry IMS were compared to concentrations measured by a phosphorous acid coated denuder for the same time period. All field data reported by an instrument prior to the calibration were then adjusted based on the trend line acquired from the calibration procedures. All the ammonia measurements used in the analysis are calibrated results, and calibrations were performed with same instrument settings and procedures in 2015

and 2016. To illustrate issues associated with the calibrations of these instruments, the calibration results from 2016 will be discussed in detail.

Calibration results in RMNP and Loveland are shown in Figure 2.2.4 Three-point calibrations were performed at both sites. The plotted values relate the calibrated concentration value (from the URG denuder) vs. the uncalibrated, raw instrument concentration output. The concentration ranges of the calibrations performed cover the majority of the ambient concentrations observed at Loveland and RMNP. A least-squares linear fit was used for the calibration curve to correct raw measurements reported by the CRDS and IMS to the URG denuder measured calibration concentrations. All three trend lines demonstrate high linearity with r^2-values all higher than 0.99. Slopes were between 0.86 and 0.98, indicating that the uncalibrated real-time instruments were modestly over-reporting ambient ammonia concentrations. This bias was corrected via the calibration procedure.

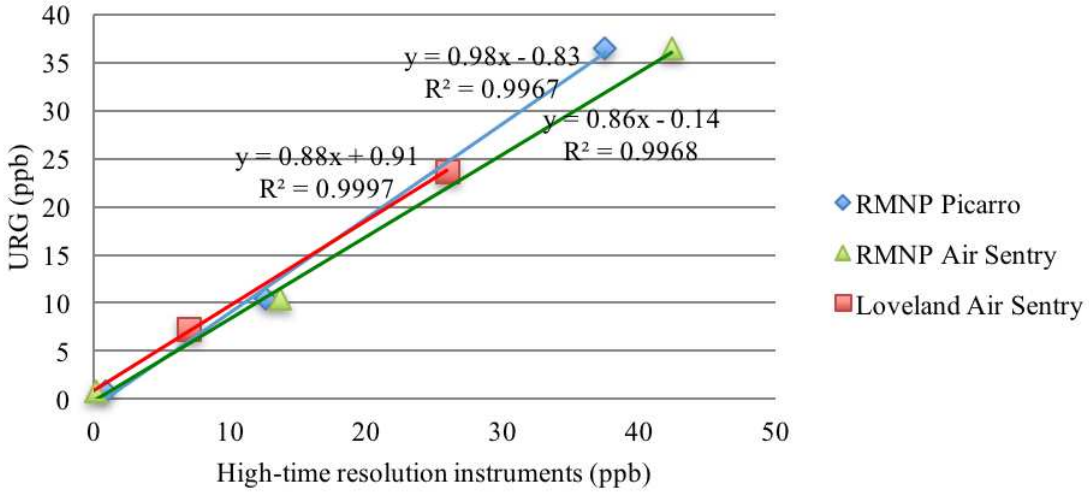

Figure 2.2.4 Calibrations for Picarro CRDS (blue diamonds) and Air Sentry IMS (green triangles) in RMNP, and Air Sentry IMS in Loveland (red squares). Blue, green and red lines are least-square fitting trend lines for each set of the data. Linear functions are indicated next to the trend lines with R^2 shown.

Measurements of ammonia in Greeley, which is closer to large ammonia sources, were calibrated for a broader range with 5 calibration points that span between 0 ppb to 200 ppb.

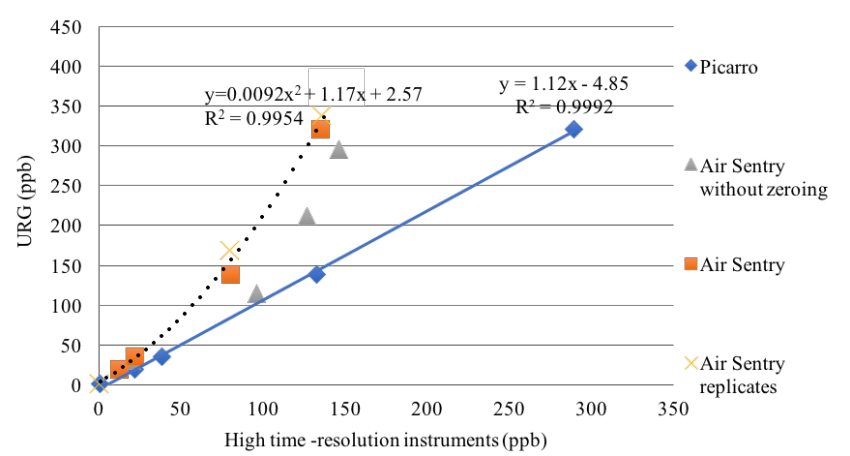

Figure 2.2.5 Calibrations for Picarro CRDS (blue diamonds); Air Sentry calibration with zero check prior to the calibration (orange squares and yellow crosses for replicates) and without zero check (grey triangles) in Greeley. The black dashed line indicates the quadratic fit line used for the Air Sentry calibration (with zero check) and the blue line indicates the calibration trend line used for Picarro measurements in Greeley.

The Picarro CRDS has a high linear response with the regression function of y=1.12 x - 4.85 with $R^2 = 0.9992$. The Air Sentry IMS is designed to measure ammonia ranges between 0 and 50 ppb which likely explains why measurements of ammonia by the Air Sentry do not appear to be linear at the higher concentrations. Therefore, instead of a linear relationship, a quadratic trend line was applied to fit the Greeley IMS raw measurement data to the calibrated values. The adjusted quadratic trend line is $y=0.0092x^2 + 1.17x + 2.57$ with $R^2 = 0.9954$. In addition, a zero/check needs to be applied to the Air Sentry IMS prior to use since changes in local pressure alter the time-of-flight and peak detection of the ion. The instrument doesn't automatically adjust for this change and will not detect the maximum of the peak and instead may detect a shoulder or tail of the peak, resulting in an inaccurate measurement of ammonia concentrations. We have observed that a positive drift may occur when calibrated for high

concentrations of ammonia as shown in the triangles that deviate from the quadratic trend line in Figure 2.2.5.

2.2.6 Mobile Ammonia Measurements

To better study the spatial variability of ammonia in NE Colorado and the characteristics of plumes emanating from CAFOs and other sources, a mobile platform with high time-resolution ammonia measurements was deployed in 2016 summer. An Air Sentry II Ion Mobility Spectrometer was operated on board a Chevrolet Tahoe for continuous ammonia measurements. The Teflon inlet tube connected to the Air Sentry ammonia monitor was heated to 102°F to minimize gaseous ammonia sticking to the tubing (OD FEP Teflon sampling line ~1m, 0.64cm) surface and the sample flow is less than 1000cc/min. A Picarro G2301 was on board the vehicle to provide GPS coordinates. Zero checks were done before the drive and a calibration was done at the end of the on-road measurements.

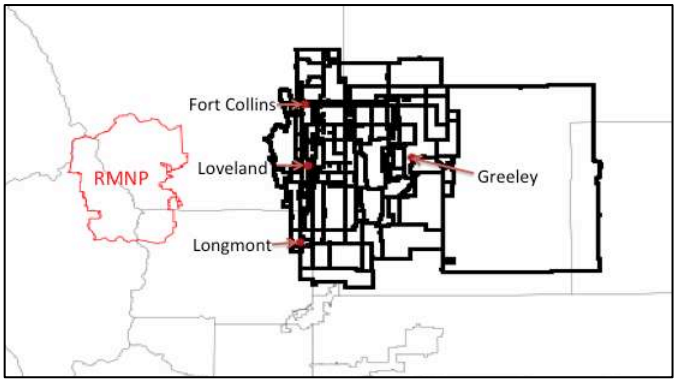

Figure 2.2.6 Selected routes of on-road ammonia measurements shown in black. RMNP is outlined in red. Fort Collins, Loveland, Longmont and Greeley are indicated by dots and pointed arrows.

The mobile platform was operated both west and east of Interstate-25 (I-25) on various highways and county roads (Figure 2.2.6). The routes include similar transects for different times

in a day and similar times on different days to gather information about the ammonia concentration diurnal pattern and the spatial variability of ammonia. The vehicle was deployed both close to the foothills of the Rocky Mountains and in regions with extensive CAFO operations. A total 99.6 hours of on-road measurements were made over 16 days with drive periods lasting from 6 to 8 hours per day. We observed that the Air Sentry ammonia monitor failed to operate properly when driven across large altitude gradients, likely due to changes in ambient air pressure that might impact the time of flight for ions inside the drift tube of IMS. Therefore, transects of ammonia concentrations were gathered from the eastern plains of Colorado to the foothills but do not reach RMNP. Other issues that occurred during some mobile measurements included power failure and failure in recording GPS coordinates.

Meteorological information was obtained from the National Centers for Environment Prediction (NCEP) 13km Rapid Refresh (RAP) model (www.rapidrefresh.noaa.gov) with hourly resolution and grid size of 13km. The RAP model provides hourly updated hybrid results of assimilated observations with model outputs. More meteorological data are available from Colorado Agricultural Meteorological Network (COAGMET) stations with hourly resolution.

The Hybrid Single-Particle Lagrangian Integrated Trajectory model (HYSPLIT) was run for select case studies with High Resolution Rapid-Refresh (HRRR) meteorological data or North American Mesoscale 12 km (NAM12) meteorological data when HRRR was not available.

2.3 Ion Chromatography

The Dionex DX-500 Ion chromatography (IC) system uses suppressed conductivity detection for determination of ion concentrations in aqueous samples. Samples are injected into

an eluent stream and ions separated as they travel through a guard column and separation column. Ion separation occurs due to interactions with the column resin based on the size and, especially, the charge of the molecule. After the ions are separated, they pass through a suppressor that reduces background eluent conductivity and then a detector that measures the conductivity. The concentration of each ion is proportional to the conductivity increase at its retention time. Calibration curves for each compound are constructed through analysis of a series of calibration standards prior to every sample analysis batch. The cation IC system for measurement of Na^+, NH_4^+, K^+, Mg^{2+}, and Ca^{2+} uses a methanesulfonic acid (MSA) eluent with a Dionex CG12A guard column and CS12 separation column and a CSRS ULTRA II suppressor, while the anion IC system (Cl^-, NO_3^-, SO_4^{2-}) uses a carbonate/bicarbonate eluent with AG14A guard column and AS14 separation column and ASRS ULTRA II suppressor.

2.4 Quality Assurance and Quality Control

For the URG denuder/filter measurements in RMNP, field blanks were collected once a week throughout the study to determine the measurement detection limits and provide blank-corrected results. Blank (no-flow) denuder/filter trains were installed on Monday and taken back to the laboratory on Wednesday. Blank denuders and filters were processed using the same extraction, storage, and chemical analysis procedures as other samples.

Laboratory blanks were collected throughout the study at least once a month for wet deposition measurements by pipetting 30 ml of DI water into a clean bucket. The blanks were then stored in clean bottles for further analysis with ion chromatography to provide detection limit and blank-corrected results. Multiple buckets were used in collection of wet deposition samples and blank corrections were done for all of them.

Zero checks were done for the high time-resolution NH_3 measurement instruments before and periodically during the sampling period. A multi-point calibration was done at the conclusion of the sampling period. The choices of calibration points vary between sites depending on local range of NH_3 concentration measurements. High time-resolution instruments in Greeley were calibrated for points of 0, 5, 20, 100 and 200 ppb, since the concentrations measured in Greeley cover a relatively broad range, while in RMNP and Loveland, 0, 5 and 20 ppb points are calibrated because the concentrations of NH_3 at these sites rarely exceed 20 ppb.

The points of various calibration concentrations were supplied through the same inlet tubing to Picarro CRDS and/or Air Sentry IMS at each site, together with a URG denuder. A trend line was then applied to the averaged concentrations measured by high time-resolution instruments to correct it for the concentration measured with the annular denuder. Linear fitting lines are created for URG denuder–Picarro comparison, and various trend lines are applied for Air Sentry measurements depending on measurement range. Field measurements were then calibrated based on the trend lines.

In the calibration system two mass flow controllers regulated flows from the Teledyne clean dry air source at the site and an ammonia gas cylinder provided by Airgas independently. Concentrated ammonia gas was diluted with clean dry air and mixed well in a glass chamber to create calibration ammonia concentrations of interest. The diluted calibration gas was then supplied to the Picarro CRDS and/or Airsentry IMS, and URG denuder. The volume of calibration gas drawn through the URG denuder was measured a dry gas meter, and samples collected for calibration follow the same extraction and IC analysis procedures as described before. High time-resolution instruments were given sufficient time (at least an hour) before

calibrating for each concentration point to ensure the calibration system output reached equilibrium.

2.5 The Early Warning System

A pilot Early Warning System has been operational since April 2014 in the eastern plains of Colorado (Piña, 2017). The voluntary participation of agricultural producers aims to reduce nitrogen emissions east of the Rocky Mountain National Park (and potentially nitrogen deposition in the park) during upslope flow events. When an impending upslope (easterly) event is forecasted, the Early Warning System informs agricultural producers by sending out warnings at least 24 hours beforehand. These warnings allow participating producers to voluntarily take actions that can lead to reduced ammonia emissions. Such actions include but are not limited to altering manure management procedures during the event, maintaining dry, clean pen surfaces, and postponement of fertilizer application for the crop producers.

A forecast model is routinely run in the Precipitation Systems Research Group at Colorado State University (http://schumacher.atmos.colostate.edu/weather/) in order to predict impending upslope events. The group uses a small ensemble of forecasts using the Advanced Research version of the Weather Research and Forecasting (WRF-ARW) model to identify transport of airflow from the NE plains of Colorado to the RMNP. The forecasts are run at 12-km spatial resolution with trajectories released from important ammonia source regions near Greeley, Limon and Fort Morgan in Colorado. Only trajectories initiated from Greeley in 2015 were used in this study due to data availability. 32 grid points are released every 3 hours per run from Greeley, and integrated forward for 6 hours.

(http://schumacher.atmos.colostate.edu/weather/real_time_wrf/traj_GXY/anim.php)

Approximately 1120 trajectories are initiated from each region per day in total but this number may be smaller due to incomplete model run or other issues with trajectory data. When trajectories travel into the RMNP receptor area, and forecasted precipitation exceeds 5mm/day, the Precipitation Systems Research Group further analyzes the model results and warnings are issued to the agricultural producers as deemed appropriate. Around 8% of days for the entire year have been identified as potentially large deposition days and warned since April 2014.

CHAPTER 3 - RESULTS

3.1 Measurements Techniques Comparison

3.1.1 Comparison of NH_3 Measurements between High-Time Resolution Instruments

Picarro CRDS and Air Sentry IMS instruments were installed in Rocky Mountain National Park from 08/10/16 to 10/12/16 and at Greeley from 08/12/16 to 09/30/16 for purposes of instrument intercomparison. The high-time resolution ammonia measurement instruments were calibrated from the same inlet at each site and calibrated results are used in the comparison. Due to the different time resolution of the Picarro (~3 sec) and Air Sentry (30 seconds) and measurement technique, the measurements were averaged to resolution of 1 minute, 5 minutes, 10 minutes, 20 minutes, 40 minutes and 1 hour for comparison and to see if there are differences in the instrument response time.

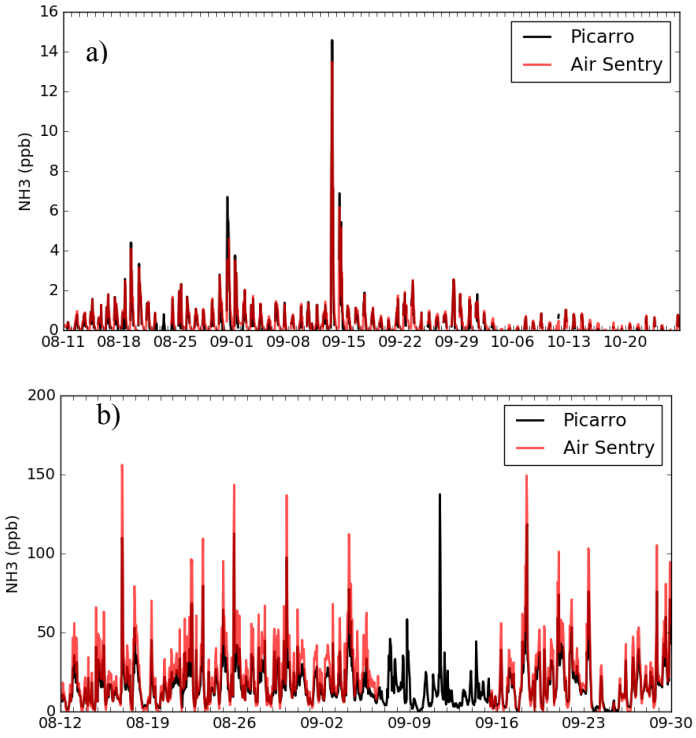

Figure 3.1.1 Temporal variations of NH_3 concentrations measured by Picarro CRDS (black) and Air Sentry IMS (red) in a) RMNP and b) Greeley in 2016.

As a first-look, Figure 3.1.1 shows the temporal variation of ammonia concentrations with 1-hour resolution in RMNP (a) and Greeley (b) for the whole overlap measuring period. Both instruments capture similar trends in ammonia concentration, whether measuring the fairly regular diurnal cycle observed at RMNP (Figure 3.1.1a) or the irregular concentration patterns observed in Greeley (Figure 3.1.1b).

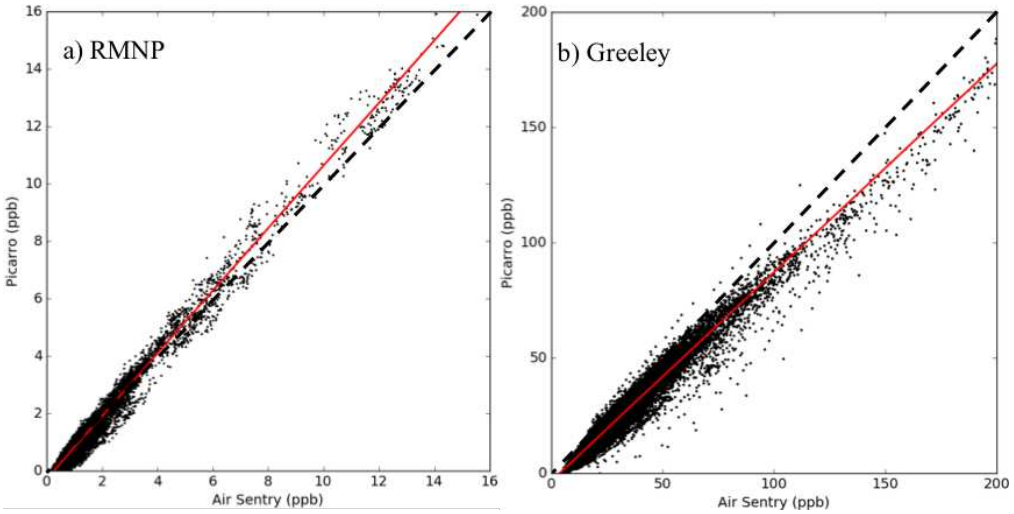

Figure 3.1.2 Correlation of 1 minute-averaged NH_3 concentrations (ppb) measured by the Picarro CRDS and the Air Sentry IMS in a) RMNP and b) Greeley. Linear trend lines are shown in red, and 1:1 ratios are shown by dotted lines.

To better demonstrate the relationship between the Picarro CRDS and Air Sentry IMS, Figure 3.1.2 shows ammonia concentrations measured by the Air Sentry plotted against measurements by the Picarro NH_3 analyzer for the same time period with time resolution of 1 minute. A least-squares fit was applied to the data, and the trend lines are shown together with the measurements. For the measurements made in RMNP, the linear trend line was Picarro (ppb) = 1.09*Air Sentry (ppb) – 0.28, with $r^2 = 0.98$, while at Greeley, the trend line was found to be Picarro (ppb) = 0.90*Air Sentry (ppb) – 3.42, with $r^2 = 0.97$.

There were minor differences observed when the data were averaged to different time scales. A summary Table 3.1.1 of least square fitting performed as measurements taken by the Air Sentry (treated as independent variable, x) and Picarro (dependent variable, y) in RMNP shows that the slope ranges from 1.07 to 1.09 and the intercept between 0.23 and 0.29, depending on the averaging time. The r^2 values are high for all comparisons with different time resolution (0.98) indicating high correlation between calibrated measurements taken by these two instruments. A small p value (0.001) indicates that the comparison results are statistically significant for all averaging periods.

Table 3.1.1 Summary table showing comparison of ammonia measurements in RMNP with various averaging time resolution ranging from 1 minutes to 60 minutes.

Time Resolution	Slope	Intercept	r^2
1 minute	1.09	-0.28	0.98
5 minutes	1.09	-0.29	0.98
10 minutes	1.09	-0.29	0.98
20 minutes	1.09	-0.28	0.98
40 minutes	1.08	-0.25	0.98
60 minutes	1.07	-0.23	0.98

A similar table is given for measurements in Greeley (Table 3.1.2). The slopes of the least squares fitting line vary slightly between 0.9 and 0.92, with the intercept ranging from 3.42 to 3.87. A slope consistently less than 1 indicates that the calibrated Picarro CRDS in Greeley measures smaller ambient ammonia concentrations than the Air Sentry monitor, which might be due to the fact that the Air Sentry IMS is sensitive to both ammonia and amines while the Picarro CRDS is only sensitive to ammonia. The Greeley site is surrounded by various types of CAFOs which can produce high emissions of both ammonia and amines (Hutchinson et al., 1982; Hristov et al., 2011). The modest bias between the two instruments might also reflect uncertainties associated with the nonlinear calibration curve for the IMS. The r^2 values higher

than 0.97 indicate high correlation by the two instruments across a large range of NH_3 concentrations. p values are 0.001 for all comparisons showing that the results are highly statistically significant.

Table 3.1.2 Summary table for comparison of ammonia measurements in Greeley with various time resolution ranging from 1 minutes to 60 minutes.

Time Resolution	Slope	Intercept	r^2
1 minute	0.90	-3.42	0.97
5 minutes	0.91	-3.46	0.97
10 minutes	0.91	-3.57	0.98
20 minutes	0.91	-3.64	0.98
40 minutes	0.92	-3.78	0.98
60 minutes	0.92	-3.87	0.98

Overall, the Picarro CRDS and Air Sentry IMS, when properly calibrated, show good agreement in ammonia concentration measurements at time resolutions as high as 1 minute and across a wide range of concentrations.

3.1.2 Comparison between Ammonia Measurements by URG Denuder/Filter Packs and High Time-Resolution Ammonia Measurement Techniques in RMNP

The URG denuder/filter packs provide information of 24-hour integrated ammonia measurements with high precision in national parks where ambient concentrations can be quite low (Benedict et al., 2013b; Benedict et al., 2013c). During 2016 daily denuder/filter-pack samples were collected in RMNP. Ammonia concentrations measured by the Picarro and Air Sentry NH_3 analyzers were averaged for URG measuring periods to match the denuder samples for comparison (Figure 3.1.3). The inlet tubing for the Picarro CRDS and Air Sentry IMS was heated to prevent ammonia from sticking inside the tube. However by doing this, semi-volatile ammonium nitrate particles may be dissociated to form ammonia, leading to higher concentrations being measured by the high time-resolution instruments compared to the URG

denuder. Therefore, the URG denuder/filter-pack total ammonia (ammonia and ammonium) is used for comparison with the high time-resolution ammonia monitors. Because particulate ammonium includes both semi-volatile ammonium nitrate and non-volatile ammonium sulfate, the resulting value should exceed the ammonia concentration that enters the continuous ammonia instruments. Figure 3.1.3 shows the trends of total ammonia concentrations in the park are well captured by all three measurement techniques, especially after mid-August 2016 when a zero calibration check was applied to both the Picarro CRDS and Air Sentry IMS. The measurements are well correlated at the lower range of ammonia concentrations (below 1 ppb), while bigger differences occur when measuring at higher concentrations. Both the Picarro CRDS and Air Sentry IMS measured the highest 24-hr averaged concentrations of ammonia on 09/14/16, where the Picarro CRDS is 6.21 ppb and Air Sentry IMS is 3.53 ppb.

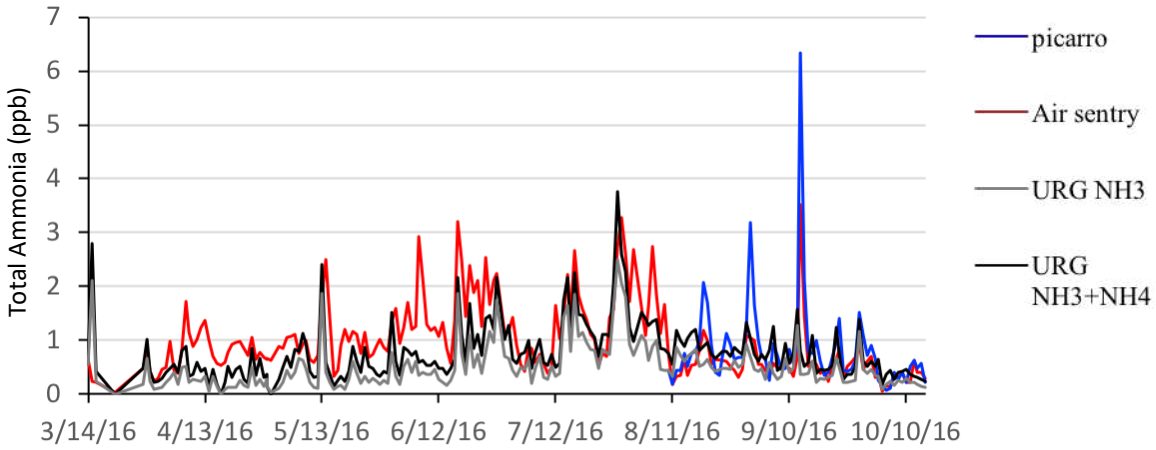

Figure 3.1.3 Daily variations of 24-hr NH_3 (ppb) concentrations measured by URG denuder/filter trains (grey), NH_3 and NH_4^+ (ppb) concentrations measured by URG denuder/filter trains (black), and NH3 (ppb) measured by the Picarro CRDS (blue) and Air Sentry IMS (red) in RMNP in 2016.

To better compare the measurements, the correlation plot with various instruments is shown in Figure 3.1.4 a). A least-squares fit model with y-intercept forced to zero is applied to compare the degree to which measurements taken by the high time-resolution instruments match

results from URG denuder/filter train measurements. Since both the Air Sentry and Picarro NH_3 analyzers are calibrated with a parallel denuder for the zero calibration point before application, it is reasonable to force the fit line through zero. The slope for both comparison is smaller than 1, with the slope for the Air Sentry-URG comparison being 0.69 and the Picarro-URG comparison being 0.48. This indicates that measurements taken by URG is smaller than the high time-resolution measurements in general. Both fit lines are skewed by measurements on 09/14/2016 when both Air Sentry and Picarro documents NH_3 concentrations higher than 3 ppb and 6 ppb respectively, while the URG measured a concentration of NH_3 lower than 2 ppb. The r^2 values are 0.54 and 0.31 for Air Sentry-URG and Picarro-URG comparison respectively, which means that the least square fitting lines explain 54% and 31% of the total variation in the measurement data by two instruments respctively. Figure 3.1.4 b) shows the ratio of total ammonia measured by URG samples and high time-resolution technique ammonia concentrations as a function of the total ammonia measured by the URG.

The comparison between high time-resolution instruments and URG denuder might have been impacted by a few factors. First, the Air Sentry IMS is sensitive to amines which cannot be distingished from ammonia, and this may introduce an overestimate of ammonia concentrations when high amine concentrations are present, although this effect is expected to be a few percent at most given the expected amine/ammonia source emission ratio and the shorter chemical lifetime of amines in the atmosphere. Second, the inlet tubing for the high time-resolution instruments were heated to minimize ammonia loss inside the inlet. Heating the tubing will lead to at least partial evaporation of semivolatile ammonium nitrate particles, producing ammonia and nitric acid gases; this will lead to a high bias in comparison of ammonia concentrations without considering disassociation of ammonium particles. In addition, the URG denuder/filter

pack is operated approximately 50 meters from the shelter where the high time-resolution instruments are located. The differing locations of the inlet for the URG and high time-resolution instruments may also cause other troubles in measuring ammonia. The inlet for the URG system is surrounded by vegetation in an open area, while the inlet for the Air Sentry and Picarro ammonia analyzers is attached to a shelter. It may be possible that shelter is a potential source for ammonia and also exchange with the surrounding air for ammonia in a different rate than the vegetations. Besides, the inlet for the continuous analyzers, while heated, might still instroduce some bias or time lags to the measured ammonia concentrations. These factors have not been tested in this measurements, and will need more targeted measurement results in future studies.

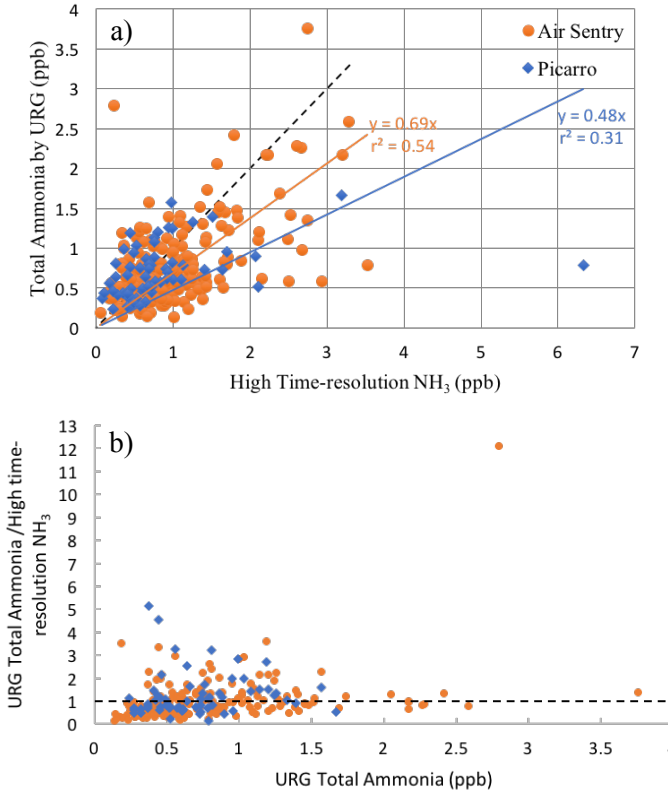

Figure 3.1.4 a) Comparison of NH_3 concentrations measured by Picarro CRDS and URG denuder/filter packs (blue); Air Sentry and URG denuder/filter packs (orange). Solid lines indicate least squares fits with intercept forced to 0. b) Variation of ratio between measurements taken by URG and high time-resolution techniques as a function of URG measured NH_3, the 1:1 ratio is indicated with doted black line.

One factor that was explored to further test possible reasons for the low bias of the URG vs. high time-resolution instrument ammonia concentrations was the order of denuders in the URG sampling train. It is standard for URG denuder trains to operate with the nitric acid absorbing denuder first in series to minimize loss of this sticky gas. In this configuration, however, part of the ammonia might be lost in transiting the nitric acid denuder before being captured by the second ammonia denuder. In the previous chapter, it was discusses that around 17% less ammonia can be captured when denuder trains are installed with the HNO_3 denuder in the first position, suggesting that ammonia concentrations measured by the reversed order denuder configuration are higher than in the normal configuration. This bias in ammonia measurement introduced from the denuder position and the degree to which this factor is influencing the comparision between measuring techniques is worth further investigation in future experiments.

In summary, fairly good agreement is observed between the two continuous instruments when properly calibrated and operating off a common inlet. Field agreement between the URG denuder/filter-pack system and the continuous instruments is not as strong. Some of this disagreement stems from the use of a heated inlet on the continuous instruments, which volatilizes at least some sample ammonium nitrate aerosol, while other inlet loss or location issues might also contribute. These data provide evidence that further work is needed to better characterize the continuous and URG ammonia measurements. It is important to determine what biases exist in either method.

3.2 Temporal Variation of Reactive Nitrogen Concentrations

Ammonia has relatively short lifetime due to deposition and reaction with other species in the atmosphere, and its concentrations may vary largely within a day due to changes in emissions or local weather patterns. The high-time resolution data needed to examine rapid changes in ammonia concentrations are not available from national monitoring networks. The Ammonia Monitoring Network (AMoN) documents ammonia measurements with time resolution of two weeks which is insufficient for observing the dynamics of ammonia concentration variability or identifying ammonia source regions (http://nadp.sws.uiuc.edu/AMoN/). The three high-time resolution monitors installed for this study (Greeley, Loveland, and RMNP) provide data that help address these issues. We can use the high-time resolution data averaged to different time scales to evaluate the usefulness of different measurement techniques with varying time resolution. For example, the diurnal concentration pattern of ammonia is useful for understanding its behavior in the atmosphere, especially as related to diurnal transport patterns, while high time resolution measurements (minutes to hours) can help identify emissions from local sources. Longer term (or more averaged measurements of high time-resolution data) can be used to study seasonal variation and long-term trends in ammonia concentrations.

3.2.1 Diurnal Cycle of NH_3 Concentrations in Greeley and RMNP Observed at High Time-Resolution

Time series of high time-resolution ammonia concentration data show that repeating diurnal cycles exist in RMNP and Greeley, although the diurnal variation patterns are different at these two sites. The ammonia concentration variation can be represented by a second order Fourier Transform with

$$\text{Diurnal cycle} = A_0 + \sum_{n=1}^{24} A_n \sin n\theta + B_n \cos n\theta$$

where $\theta = \frac{\pi t}{12}$ and $0 \leq t \leq 24h$ (Carson, 1963). The Fourier transform reduces a concentration-time curves to a series of Fourier coefficients and helps to capture the main character of ammonia variation over the course of a day. 2015 observations for both Greeley and RMNP sites were Fourier transform fitted separately by month and results are shown in Figure 3.2.1.

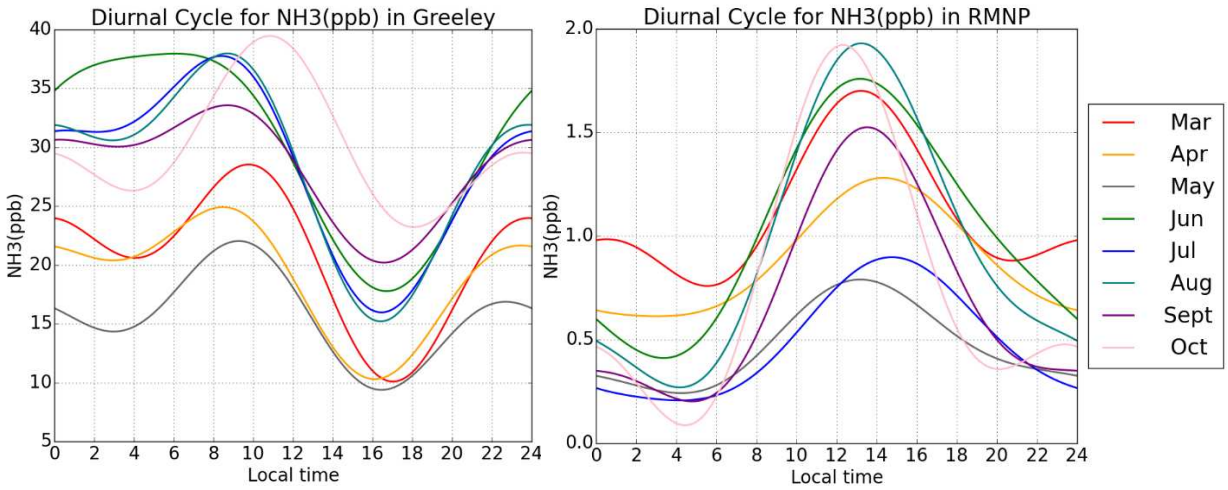

Figure 3.2.1 Fourier transformed series of NH_3 (ppb) diurnal cycle in Greeley and RMNP from March to October, 2015.

In this figure, we can see that ammonia concentrations in Greeley build up after sunset, followed by a rapid decrease after sunrise. Since Greeley is within a region of intense ammonia emissions, the diurnal cycle is likely related to the atmospheric boundary layer diurnal evolution. At sunrise, heating from below increases vertical mixing and grows the boundary layer; this facilitates pollutant dilution. A more stagnant environment often forms during night associated with a thin nocturnal boundary layer (Garratt, 1992) and prevents local ammonia emissions from spreading out and diluting. Compared to Greeley, RMNP is a much more pristine environment absent major agricultural and vehicular ammonia emission sources, so that transported ammonia

largely drives the local diurnal ammonia concentration variation. Toth and Johnson (1985) have shown that RMNP and northeastern Colorado are strongly influenced by terrain effects. A diurnal wind pattern similar to classic mountain-valley circulations dominates transport on many days. Solar heating of the east slope of the Rockies induces easterly winds during the daytime, especially (but not exclusively) in summer. Previous studies in RMNP observed that from daybreak, the terrain-driven easterly flow leads to increase of ammonia in RMNP that is associated with the transport of pollutants from the eastern plains of CO, while downslope flow at night flushes the site with clean air that decreases local ammonia concentrations (Malm et al., 2013). Other processes can contribute to the diurnal concentration cycles, including: bi-directional ammonia exchange with vegetation (Sutton et al., 1995), temperature-dependent emissions from soil (Potter et al., 2003), and uptake and re-emission of ammonia by dew (Wentworth et al., 2016). The month to month diurnal ammonia concentration cycle is similar at each site in terms of pattern, whereas absolute values vary largely among seasons and months, mainly due to emissions changes and meteorological impacts, such as transport, vertical stability, precipitation and temperature. As shown in Figure 3.2.1, ammonia concentrations in June, July and August (with averaged daily high temperature of 32.7 °C) in Greeley are much higher than the diurnal cycle peak generated for March, April and May with averaged daily high temperature of 19.8°C. This partly reflects the fact that ammonia emissions increase with temperature while high temperature also helps facilitate dissociation of ammonium nitrate particles to release ammonia gas. The diurnal cycle of ammonia concentrations in RMNP did not show a clear seasonal pattern, which may reflect the fact that ammonia transport to RMNP is largely influenced by meteorological factors other than temperature, including wind fields and precipitation. Earlier work (Benedict et al., 2013c) has shown that RMNP ammonia

concentrations in midwinter (a time period not studied here) are much lower because the park is meteorologically more isolated from ammonia emissions at lower altitudes.

3.2.2 Seasonal Pattern of Reactive Nitrogen Concentrations in RMNP Observed by URG Denuder/Filter Trains in 2015

Daily URG denuder/filter measurements in 2015 were used to study the seasonal variation (spring to fall) of reactive nitrogen gas and particle concentrations in RMNP. Monthly data were pooled to examine mean concentrations and percentile information. Figure 3.2.2 shows monthly variation of gaseous ammonia and nitric acid, together with particulate ammonium and nitrate concentrations.

Variation of gaseous ammonia concentration has a clear seasonal pattern. The concentration peaks in August with median 24 hr value of 0.35 $\mu g/m^3$, while the lowest monthly mean and median NH_3 concentrations were observed in May. This can be explained by the fact that May has much more precipitation amount than other months of interest in 2015, with average daily precipitation of 3.83 mm, followed by July with 2.9 mm/day. Precipitation scavenging has been shown to be an efficient pathway for ammonia removal from the atmosphere (Shimshock et al., 1989; Crutzen et al., 2000; Mizak et al., 2005), and the lower average ambient ammonia in May, and even July may be attribute to precipitation wash-out. The peak of ammonia in August may be associated with high temperature in the month. The average monthly temperature reaches maximum in August (14.79 °C), coinciding with when the highest monthly ammonia concentration was observed. High temperature facilitates the decomposition of particulate ammonium nitrate into gaseous ammonia and nitric acid (Stelson and Seinfeld, 1982; Mozurkewich et al., 1993), and it may also result in higher ammonia emissions from the sources, such as agricultural activities (Sommer et al., 2001; Pagans et al., 2006) and fertilized

soils (Sommer et al., 2004). Reduced precipitation and continued strong solar heating that drives upslope transport from agricultural sources to the east may also have contributed to increased ammonia concentrations in August. The observation reveals a similar seasonal pattern to a previous study (Benedict et al., 2013c) showing that ammonia concentrations increase beginning in the spring and are higher during the summer.

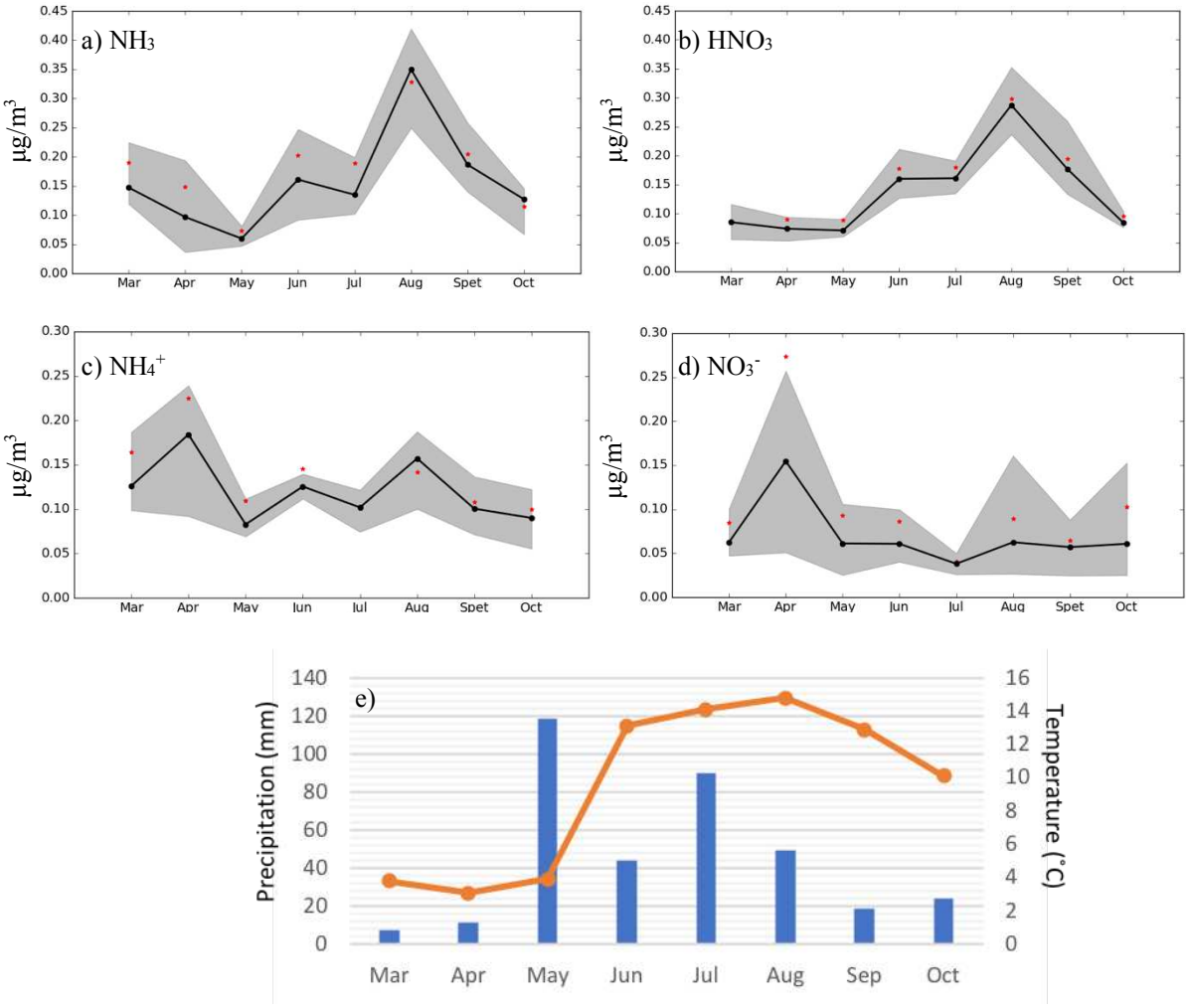

Figure 3.2.2 Monthly variation of a)NH_3 b)HNO_3 c)NH_4^+ d)NO_3^- concentrations ($\mu g/m^3$) and e) precipitation (mm) and temperature (˚C) from March to October in RMNP in 2015. 25th and 75th percentiles are shown by the shaded area. Dotted black line indicates median concentration of the month. Red stars indicate monthly mean values.

The variation of nitric acid concentrations follows a similar pattern as ammonia gas, with maximum monthly mean of 0.30 μg/m^3 in August. The nitric acid concentration level is expected to be higher in the summer with more intense photochemical reactions that resulted from longer daytime and higher sun's zenith angle. In addition, higher temperatures in summer also help to increase the HNO_3 concentration by accelerating the dissociation of NH_4NO_3 into gas phase HNO_3 and NH_3.

Ammonium and nitrate in $PM_{2.5}$ is higher in April than other months, with averaged monthly concentrations of 0.23 μg/m^3 and 0.27 μg/m^3 respectively. Particulate NH_4^+ shows less variation across different months than other compounds, whereas NO_3^- concentration has a distinct peak in April and returns to the March values with little variation after that. The formation of NH_4NO_3 (p) is impacted by various factors, such as ambient temperature, humidity, abundance of ammonia gas. In general, NH_4^+ concentrations increase together with NH_3 concentrations in Rocky Mountain National Park. When ammonia concentration peaks in August, the particulate ammonium concentration also shows an increase. Monthly mean particulate NO_3^- concentration reaches maximum in April and keeps relatively low after May 2015. The formation of NO_3^- is not favored under low relative humidity and high temperature, which is the case in summer.

3.2.3 Seasonal Pattern of Ammonia Concentrations in Greeley and Loveland Observed by High Time-Resolution Instruments

Measurements of ammonia made with the Air Sentry II ammonia analyzer in 2016 are used here to study the monthly variation pattern. Figure 3.2.3 shows that ammonia concentrations vary by month at the Greeley and Loveland sites. The NH_3 concentrations in Greeley peak in June, with monthly mean of 30.1 ppb and stayed high for the rest of the

measuring period. The lowest level of ammonia is observed in May with monthly mean of 15.0 ppb and less variation during that month. The low NH_3 concentrations in Greeley in May 2015 can be attributed to precipitation scavenging of ammonia in the regional atmosphere, since May is the month with the highest precipitation amount during the measurement time. Comparing to

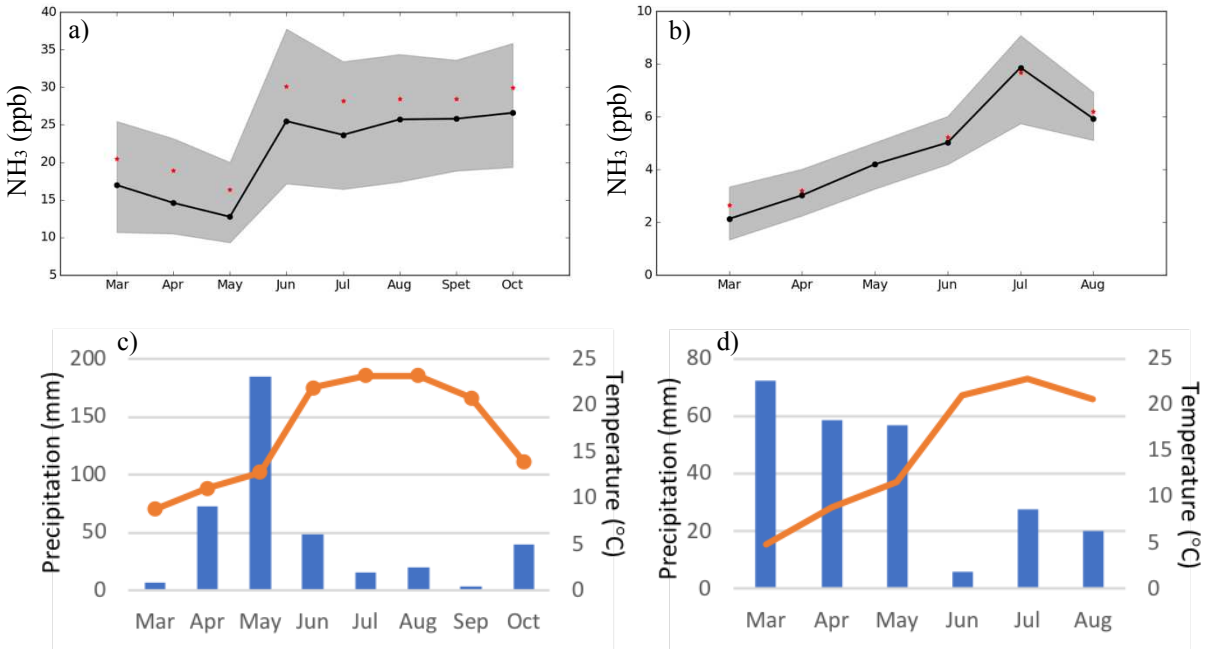

Figure 3.2.3 Monthly variation of median NH_3 (ppb) (black line) from March to October in a) Greeley and b) Loveland. 25th and 75th percentiles are shown in the shaded area. Dotted black line indicates median concentration of the month. Red stars indicate monthly mean values. Monthly variation of averaged temperature (°C) and precipitation (mm) are shown in panels c) Greeley and d) Loveland.

the monthly variation of ammonia concentrations seen in RMNP, it is found that ammonia concentrations are largely impacted by precipitation and temperature at RMNP, with lower level of ammonia in months with low temperature and high precipitation. The overall concentrations of ammonia gas are much higher in Greeley than at Loveland and RMNP, consistent with Greeley's proximity to many Confined Animal Feeding Operations and other agricultural sources. The monthly averaged ammonia concentration in Loveland kept increasing from March and reached maxima in July 2016, with an averaged concentration of 8.0 ppb in July. The

seasonal variation has the same pattern as the temperature variation observed in Loveland site, with March being the lowest and July being the month with highest temperature during the measuring period.

3.3 Spatial Distribution of NH_3 in RMNP and NE Colorado

It has been shown in chapter 3.2 that the diurnal cycle and seasonal variation of measured ammonia in Greeley differs from Loveland and RMNP. Beyond temporal variability, spatial variations of ammonia concentrations will also be investigated using high time-resolution measurement techniques, both in-situ and on-board a mobile platform. These observations will help characterize the distribution of ammonia in NE Colorado, and aid identification of major ammonia sources in the area.

3.3.1 West-East Gradient of Ammonia Concentrations in RMNP and NE Colorado

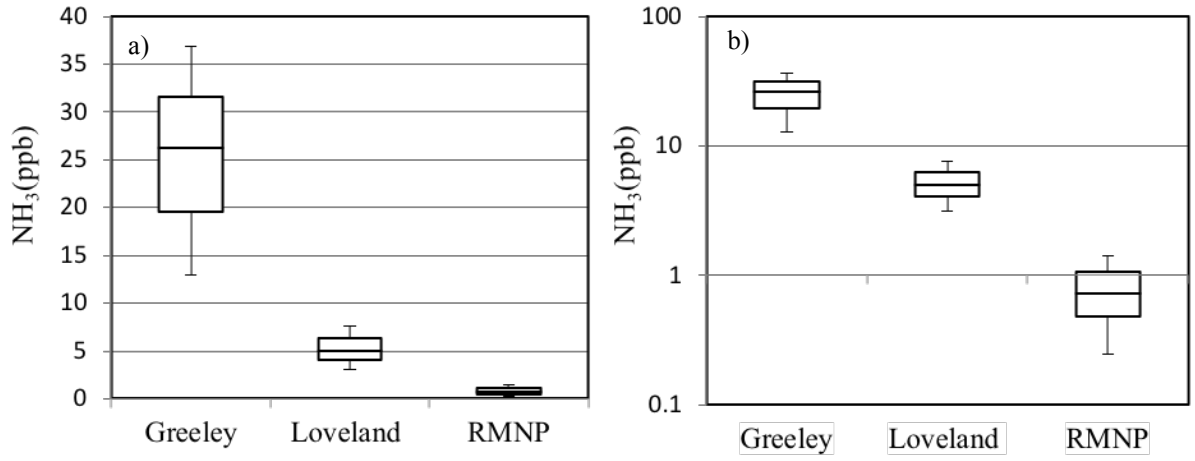

Figure 3.3.1 Plots of 25th percentile, median and 75th percentile of daily averaged NH_3 concentrations (ppb) in Greeley, Loveland and RMNP in 2016 plotted on a) linear scale and b) log scale.

Continuous measurements of high time-resolution ammonia concentrations are available from RMNP, Loveland and Greeley from March to October, 2016. Daily averaged ammonia concentrations were compared across the three sites to analyze the spatial distribution. Strong east-west gradients of ammonia concentrations are observed in NE Colorado. Being adjacent to agricultural source regions, Greeley has the highest ammonia concentrations of all three sites. The median value of daily averaged NH_3 Greeley is 26.2 ppb, much higher than 6.3 ppb in Loveland and 0.97 ppb in RMNP. Ammonia concentrations measured in Greeley site also show a higher standard deviation than the other two sites. As shown in Figure 3.3.1, the difference between the 75^{th} and 25^{th} percentile values in Greeley is 12.0 ppb, while for Loveland the difference is 2.2 ppb and for RMNP it is 0.58 ppb.

3.3.2 Spatial Variability of Ammonia Concentrations NE Colorado Observed from a Mobile Platform

To better characterize the spatial variability of ammonia concentrations in the Front Range, and provide insights into transport of ammonia plumes into the park, a mobile platform was deployed in June 2016 to measure ammonia gas concentrations in northeastern Colorado. The on-road measurements of ammonia were designed to measured ammonia concentrations with high time and spatial resolution in the northeastern plains of Colorado, and characterize whether ammonia is transported from the source regions via distinct plumes that could produce deposition hotspots upon reaching the mountains or whether distinct initial source plumes merge to form a more homogeneous larger source region plume that would deliver more uniform ammonia concentrations to the foothills to the west.

Table 3.3.1 summarizes the ammonia concentrations and some meteorological conditions for each driving day. The meteorological conditions are taken from a Colorado Agricultural

Meteorological Network (COAGMET) weather station 2.5 miles NE of Greeley (GLY03). Selected ammonia measurements were omitted due to issues encountered during the on-road measurements, such as failure of the Picarro instrument recording GPS coordinates, drift in ammonia concentrations measured by the Air Sentry monitor likely caused by drastic change in ambient pressure (which can affect the time of flight inside the IMS drift tube), power outage to the instruments, and inadequate supply of zero air to the Air Sentry NH_3 monitor.

Table 3.3.1 Summary for NH_3 measurements and weather conditions for each drive period. Drive Notes are given for days with incomplete or missing data. * Part of the meteorological data are missing for Greeley.

Date	Start time	End time	Average NH_3 Concentration (ppb)	GLY03		
				Average Temperature (°C)	Average Wind Speed	Notes
06/07/2016	10:02	14:32	30.09	25.84	2.91	
06/08/2016	10:18	14:58	22.62	--	--	RMNP
06/09/2016	8:50	16:37	16.06	30.75	1.40	
06/10/2016	9:23	13:49	14.58	16.83	2.12	GPS issue
06/13/2016	9:13	14:45	19.55	--	--	RMNP
06/14/2016	10:02	12:18	13.72	23.43	1.19	
06/15/2016	10:37	16:04	49.65	27.92	1.79	
06/16/2016	10:00	16:04	26.74	30.73	1.97	
06/17/2016	9:32	16:10	20.29	29.03	3.51	
06/20/2016	9:39	16:13	19.52	24.57	2.62	
06/21/2016	9:09	17:04	24.95	29.60	2.24	
06/23/2016	9:26	16:20	16.95	28.68	2.49	
06/24/2016	9:40	15:33	31.87	31.07	2.16	
06/27/2016	8:48	16:03	24.43	28.69*	1.97*	
06/28/2016	9:25	16:14	40.84	27.88	1.66	
06/29/2016	9:51	16:31	28.81	26.40	1.47	

The average ammonia concentrations for the driving periods range from 13.7 ppb to 49.7 ppb, with large spatial variability for measurements made in a single day (Table 3.3.1). In addition to a strong influence of source proximity, higher ammonia concentrations are generally associated with lower wind speeds and higher temperatures. The on-road measurements were

conducted at a slightly different time each day, and various routes and drive distances were taken, so that the average measurements of ammonia concentration are not the best indicator for showing the measurement results.

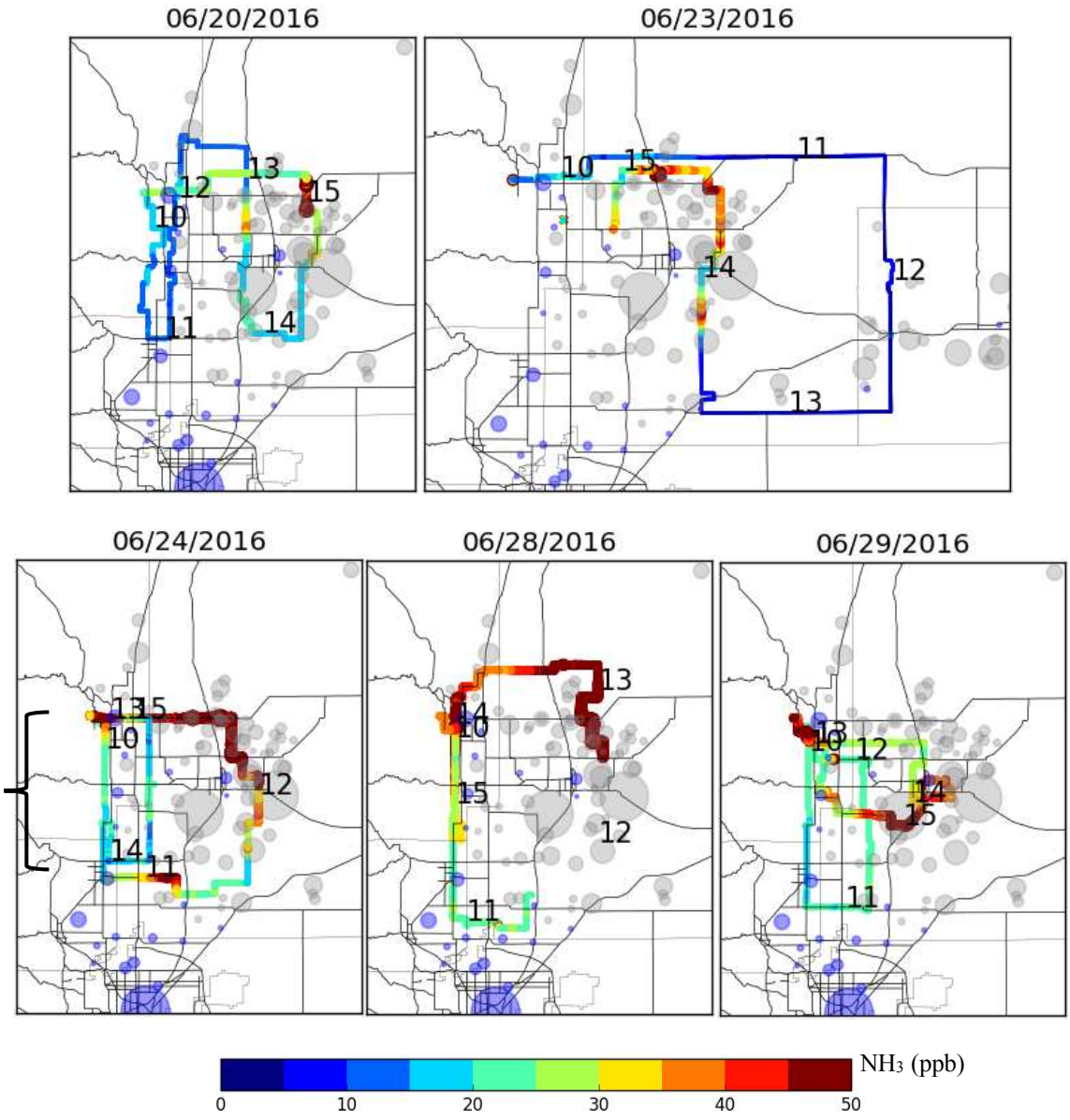

Figure 3.3.2 Mobile measurements of on-road ammonia on 20th, 23rd, 24th, 28th, 29th in June 2016. The colored line indicates driving routes with hour of the day marked by the side. Grey dots indicate CAFOs scaled to maximum animal units allowed. Blue dots indicate waste water treatment plants (WWTP) scaled by designed flow (millions of gallons per day (MGD)). The maximum designed flow of the WWTP in Denver is 220 MGD.

Figure 3.3.2 shows spatial distribution of ammonia concentrations on 5 selected measurement days. Mobile measurements usually start at the CSU Department of Atmospheric Science in west Fort Collins around 9:00 in the morning and end in the afternoon at the same location. The on-road measurements of ammonia are overlaid with locations of Confined Animal Feeding Operations (CAFOs) and Waste Water Treatment Plants (WWTP). The CAFOs are scaled between 230 to 125150 animal units, while the WWTPs are scaled by the designed flow up to 220 million of gallons per day. The highest ammonia concentration, encountered close to feedlots in the Greeley area, exceeded 100 ppb, while the lowest concentration was below 5 ppb. The ammonia concentration hotspots on drive routes in Figure 3.3.2 are found close to CAFOs and Greeley. For example, the highest concentration was observed near CAFOs by Galeton, CO in the afternoon near 15:00 on the 20th June. Hotspots were also observed in the same area on the 23rd, 24th, and 28th of June. On 24th June high concentrations of ammonia were also observed between 12:00 and 13:00 on Highway 14 where various feedlots are located.

To better quantify the spatial distribution of ammonia concentrations in the Front Range, all available and valid on-road measurements in June 2016 were selected for analysis. Figure 3.3.3 a) demonstrates all available driving routes that lie within 15km of our measurement site in Greeley; the selected region also covers the air parcel trajectory starting points in Greeley in the model operated for the Early Warning System (see the next section). The distributions of observed ammonia concentrations within and outside this defined Greeley area are also plotted in Figure 3.3.3 b). Ammonia measured within 15 km of Greeley has a lowest concentration of 16 ppb, and is missing the lower end of the distribution observed outside the Greeley region. The mean concentration of on-road ammonia near Greeley is 38.4 ppb, compared to the averaged value measured outside of the range of 24.0 ppb. Of course, these more distant locations are

sometimes downwind of Greeley and see impacts of CAFO emissions in that region. The lower tail of the non-Greeley measurement distribution shows that much cleaner conditions are also experienced at those sites.

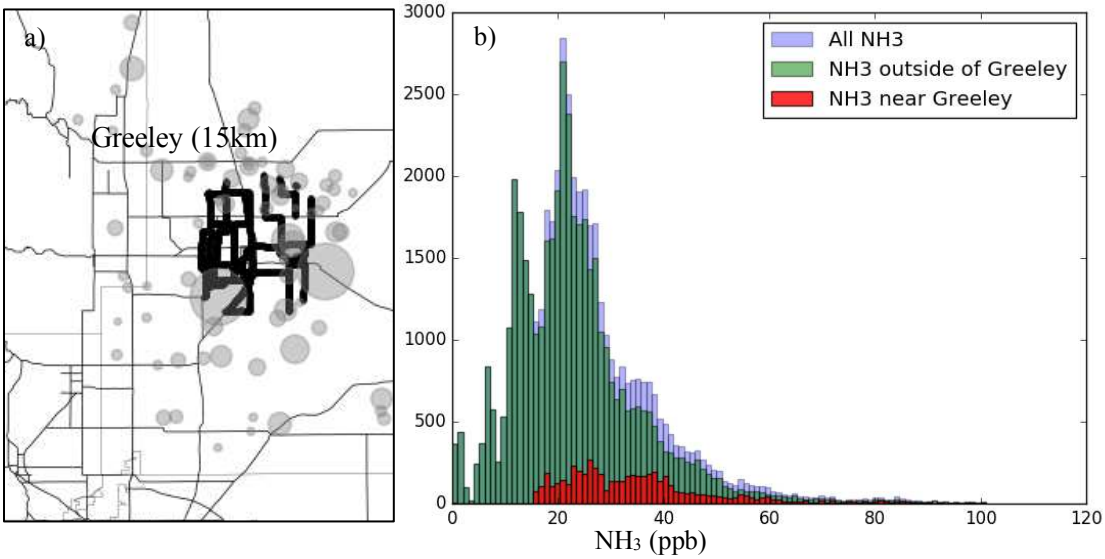

Figure 3.3.3 Maps of driving routes and with available measurements within a) 15km of Greeley center. Distribution of ammonia concentrations (ppb) within b) 15km of Greeley center (red), Green shows concentrations outside of 15km range of Greeley, Blue is the distribution of all on-road measured concentrations.

To better study how wind fields are impacting the transport and distribution of ammonia in a given day, north-south cross sections were selected for analysis with meteorological output from the National Center for Environment Prediction (NCEP) 13km Rapid Refresh (RAP) model (http://rapidrefresh.noaa.gov/). RAP provides hourly updated hybrid results of assimilated meteorological observations with spatial resolution of 13km. Similar transects were driven at both 10:00 and 13:00 on June 24th as indicated in Figure 3.3.4, shown here together with wind fields generated by RAP for the hour. The variation of ammonia for these two transects with latitudes is also shown. It is observed that the highest concentration of ammonia was found at the south end of the transect at 10:00 near Longmont, shifting to the north near Fort Collins at 13:00. Low wind speed is shown in the wind field at 10:00 near Longmont, indicating stagnation

condition at the area. This corresponds to the high concentrations of ammonia near 40.37°N that may be associated with less mixing and movement of the local air. The wind later the same day at 13:00 is faster and the wind direction close to the CAFOs is from the southeast. Transport of ammonia from the source regions near Greeley appear to contribute to high ammonia concentrations at the north end of the cross section. The change in spatial distribution of ammonia indicates that meteorological conditions, mainly wind speed and wind direction, play an important role in determining spatial variation of ammonia in the Front Range.

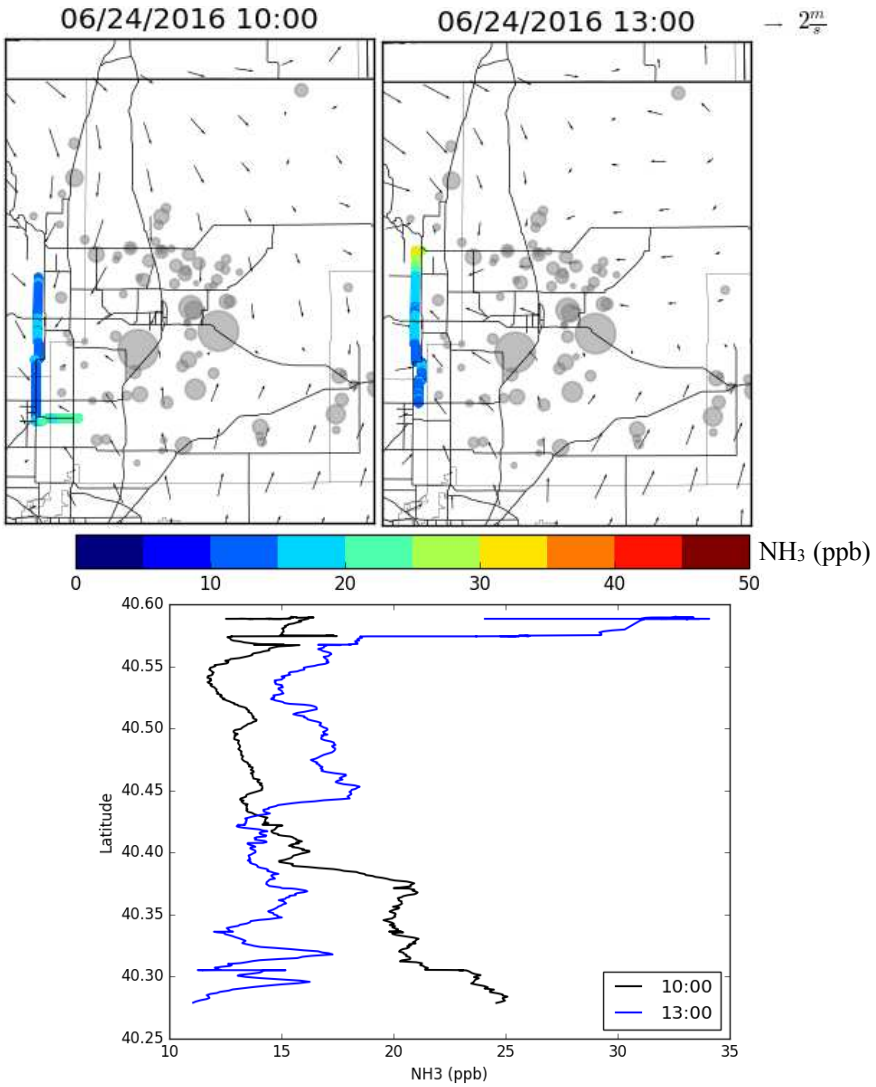

Figure 3.3.4 Mobile measurements of ammonia (ppb) at 10:00 and 13:00 on 24th June. The ammonia concentration as a function of latitude is shown in lower panel.

Model results from the Hybrid Single Particle Lagrangian Integrated Trajectory Model (HYSPLIT) (https://ready.arl.noaa.gov/HYSPLIT.php) are incorporated in the on-road ammonia measurements for studying transport of ammonia from the source regions. HYSPLIT 6-hour back trajectories were run at each hour with initial coordinates from the driving route.

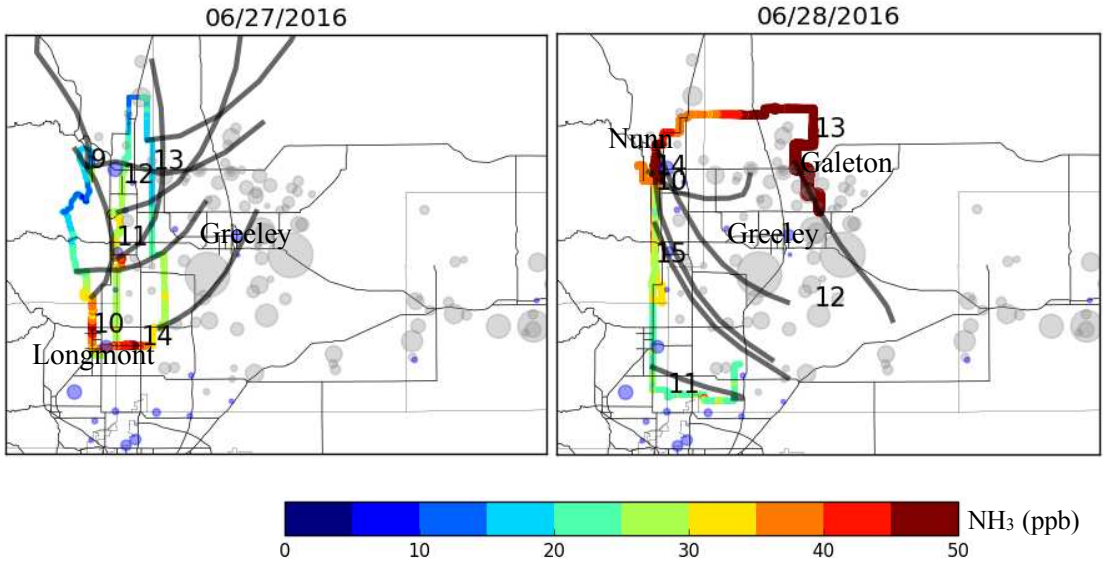

Figure 3.3.5 Mobile measurements of ammonia on 27th and 28th June with HYSPLIT 6-hour back trajectories on each hour initiated from the vehicle location.

Two examples were chosen to illustrate transport of ammonia from the source regions in Figure 3.3.5. Trajectories for these two selected cases were found close to ground level. Dominant transport is from the northeast on 27th June, while early morning transport (before 9:00) is from the northwest. Concentrations of ammonia were highest near Longmont, which is downwind of large feeding operations in Greeley. A pronounced north-south concentration gradient exists on this day with higher values to the south and lower concentrations to the north. This contrasts with the north-south gradient on 28th June which shows the opposite trend. On June 28th, high concentrations are observed near Fort Collins, Nunn and Galeton, while lower concentrations were found at the south end of the driving route. HYSPLIT 6-hour back

trajectories show northwest transport from the CAFOs in Greeley to the downwind regions in Fort Collins, Nunn and Galeton.

3.4 Transport of Reactive Nitrogen from NE Plains of CO to RMNP

3.4.1 Wind Roses and Terrain Features

To study the degree to which transport plays a role in influencing the ammonia concentrations at Rocky Mountain National Park, Loveland and Greeley, we have performed a series of analyses to understand the relationships between wind fields and ammonia concentrations. Local wind roses and conditional probability function analyses were performed for each of the research sites with measurements of high time-resolution NH_3. Since the meteorological data have time resolution of an hour, hourly-averaged ammonia concentrations were used in the analysis. The measurements periods are representative of late spring and summer as they cover April to the end of September. Since measurements of NH_3 were not available in Loveland site until late July in 2015, only measurements in 2016 are used in our analysis.

To illustrate the local wind pattern at each site, wind roses showing the relative frequency distribution of wind direction are given in Figure 3.4.1. Winds are most often from the northwest in RMNP, followed by a second maximum from southeast. There is a sharp decrease in wind frequency when deviating from these directions due to a channeling effect of local topography surrounding the site (Figure 3.4.2). The wind speed in RMNP site is typically below 4 m/s and rarely exceeds 6 m/s. The southeasterly wind, with the local channeling, reflects upslope transport from the eastern plains of Colorado. The wind roses are plotted separately for daytime (07:00 – 19:00) and nighttime (19:00 – 07:00 (+1 day)) for further analysis. In Rocky Mountain

National Park, it is observed that during the daytime, winds blow most often from the southeast, while winds at night are primarily downslope from the northwest. This is what one would expect at this site, especially in summer, when winds are strongly influenced by a mountain/valley diurnal circulation.

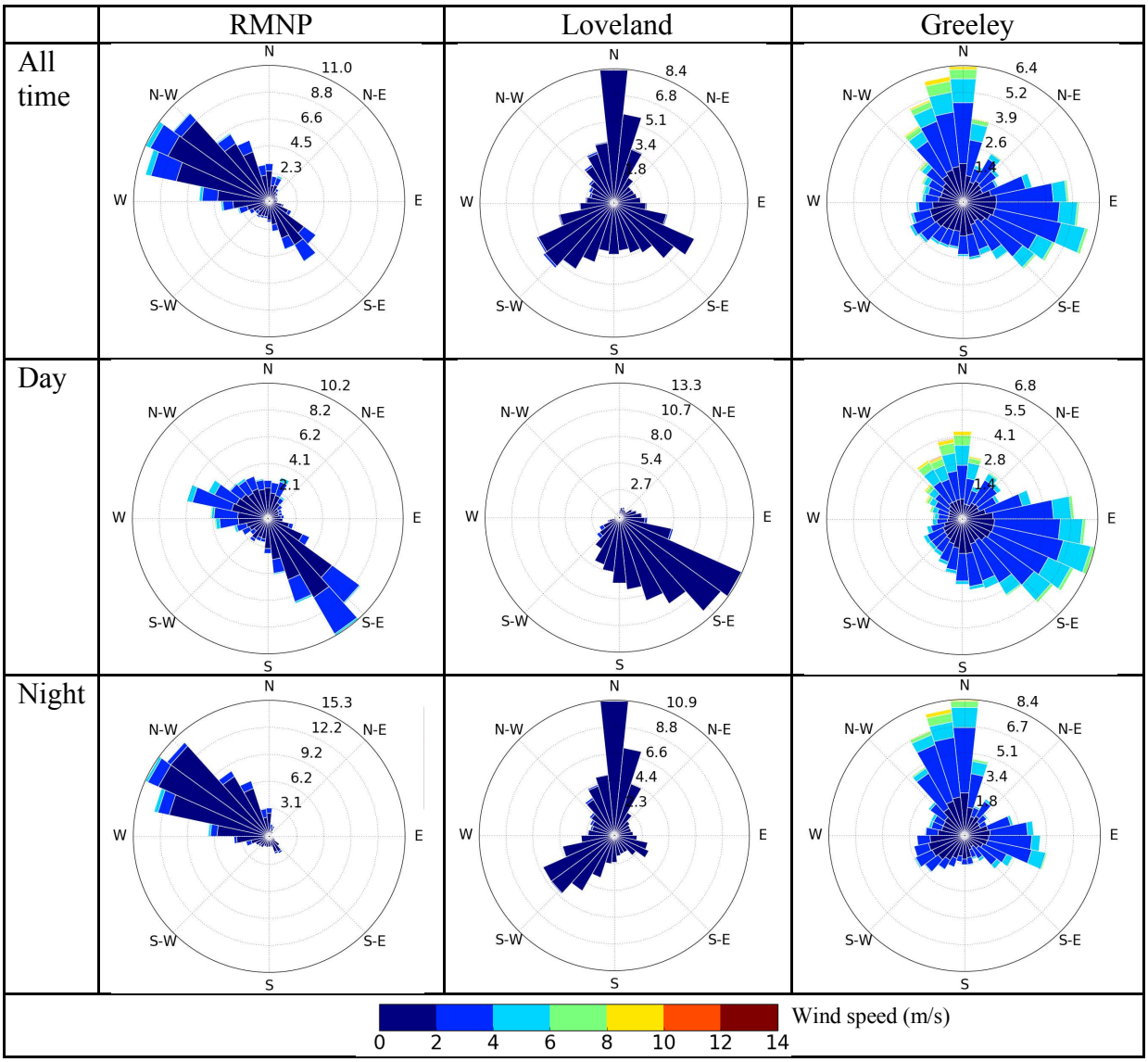

Figure 3.4.1 Wind rose showing the frequency and speed of wind at each measurement site. Each column shows wind roses in RMNP, Loveland and Greeley respectively. Rows show wind roses for the whole day, only during the daytime (07:00 – 19:00), and only during nighttime (19:00 – 07:00 (+1 day)). The length of spoke represents the relative frequency of wind coming from given wind sector. Each spoke is divided by color into wind speed ranges.

During the day, sun heats up the eastern slope of the rocky mountain, warming the air in contact with the surface, and that warm air ascends. By contrast, strong radiative cooling of the mountain slope at night leads to surface (and adjacent air) cooling, producing downslope drainage flows. At the RMNP study site, local topography channels the upslope/downslope flow from the southeast/northwest.

The Loveland site is located at the foothills of the Rocky Mountains east of RMNP (see map in Fig 3.4.2). The dominant winds at the Loveland site are northly wind, southwesterly and southeasterly wind. This also corresponds to a local mountain breeze/valley breeze pattern considering the topography features of the site. Winds blow most often from the southeast direction during the daytime, corresponding to upslope flow from the northeastern plains of Colorado, while northerly and northwesterly winds are dominant during the nighttime. Wind speeds at the Loveland site are particularly low, rarely exceeding 2 m/s, lowest among the three NH_3 measurement sites. This may mean that ammonia concentrations at the Loveland site are more locally impacted even with changing wind directions.

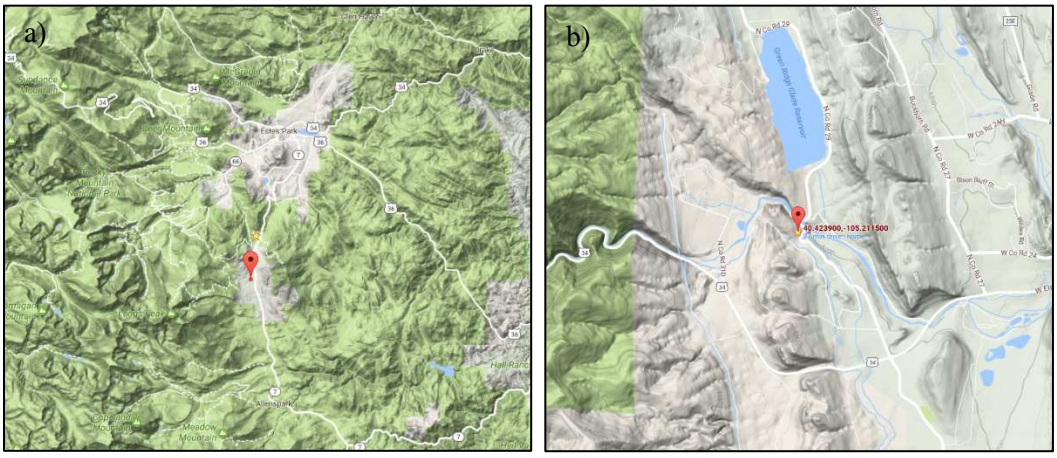

Figure 3.4.2 Topographic map for the areas around a) RMNP site and b) Loveland. Measurement sites are marked in red.

The Greeley wind rose shows that winds blow more often from the north/northwest and southeast, and higher wind speeds are usually associated with winds blowing from these two directions. The wind directions in Greeley follow a similar diurnal pattern as at the other two sites, although greater variability in wind direction is observed, likely due to Greeley's distance from the mountains and greater influence from synoptic flow. A small fraction of winds often blows from the southwest during the nighttime, and since a large feedlot is located less than 10 miles southwest of Greeley, this is likely one contributor, along with reduced mixing heights, to the higher concentrations of NH_3 measured at night in Greeley.

3.4.2 Conditional Probability Functions

Conditional probability functions have been widely applied in studying source apportionment of various atmospheric compounds (Ashbaugh et al., 1985; Kim et al., 2004) since only meteorological data and concentrations are needed for the analysis. The conditional probability functions provide a connection between elevated pollutant concentration periods and the wind field, and are commonly used to estimate the potential for a source or source region to contribute to high periods of local pollutant concentrations. The 90^{th} percentile conditional probability function (CPF) is calculated by comparing the number of concentration measurements above the 90^{th} percentile to the total number of concentration measurements in a given 10-degree wind sector. Here we perform that calculation for each of the three measurement sites (Figure 3.4.3) to examine from which direction high concentration ammonia air most likely originated.

High concentrations of NH_3 in RMNP (Fig. 3.4.3 a) are related to wind blowing from the southeast direction, corresponding to upslope transport from the Front Range and eastern plains

of CO. This is what one would expect since the intensive agricultural activities in the region east of RMNP are important sources for ammonia emission. In Loveland, higher concentrations of NH_3 are observed when winds are blowing from the northeast and southwest directions (Fig 3.4.3 b). The northeasterly upslope wind may bring airflow from the northeastern plains of Colorado to the site while the southwesterly winds could be associated with downslope transport of high concentration air masses previously transported upslope in the daytime. The Loveland wind rose (Fig 3.4.1 c) shows this site has a strong diurnal cycle, with downslope westerly wind almost every night, although the overall wind rose is dominated by NW winds while the CPF is dominated more by SW winds. Figure 3.4.3 c shows the 90th CPF function for Greeley. The conditional probability function in Greeley is more evenly distributed in all directions, with some skewing to transport from the south. The more even distribution of the CPF likely reflects the fact that the Greeley site is surrounded by various active agricultural sources of NH_3. A large cattle feedlot located less than 10 miles southwest of the Greeley site may be responsible for the southern CPF skew. In addition, wind speeds associated with the southwesterly winds are much lower than for all other directions, resulting in less dilution of emissions from that direction.

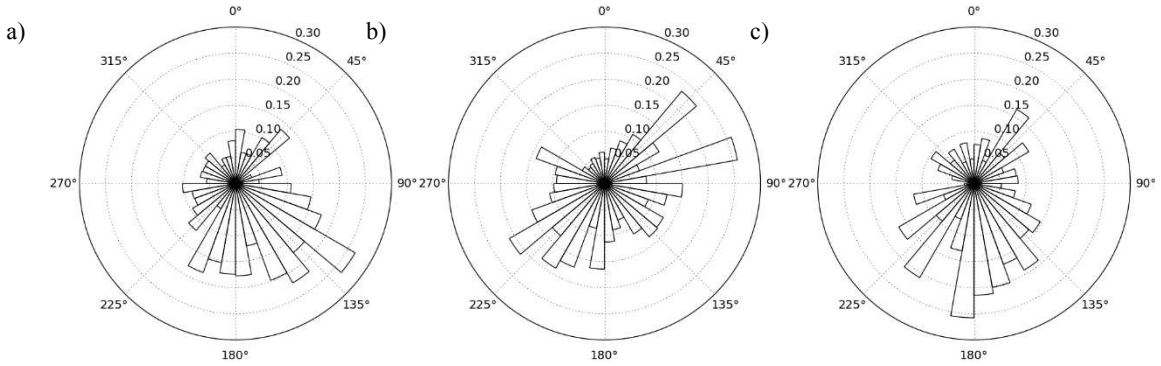

Figure 3.4.3 90th percentile conditional probability function for NH_3 at a) RMNP b) Loveland and c) Greeley.

3.4.3 Case Analysis of Transport of NH_3 by Upslope Winds

The high time-resolution ammonia measurements available at these three sites across NE Colorado potentially allow one to examine gradients in measured ammonia concentrations and characterize how upslope easterly flow contributes to transport of ammonia from the source regions to RMNP. An upslope case was selected, in order to examine how upslope easterly transport contributes to increased ammonia concentrations in the park (Figure 3.4.4).

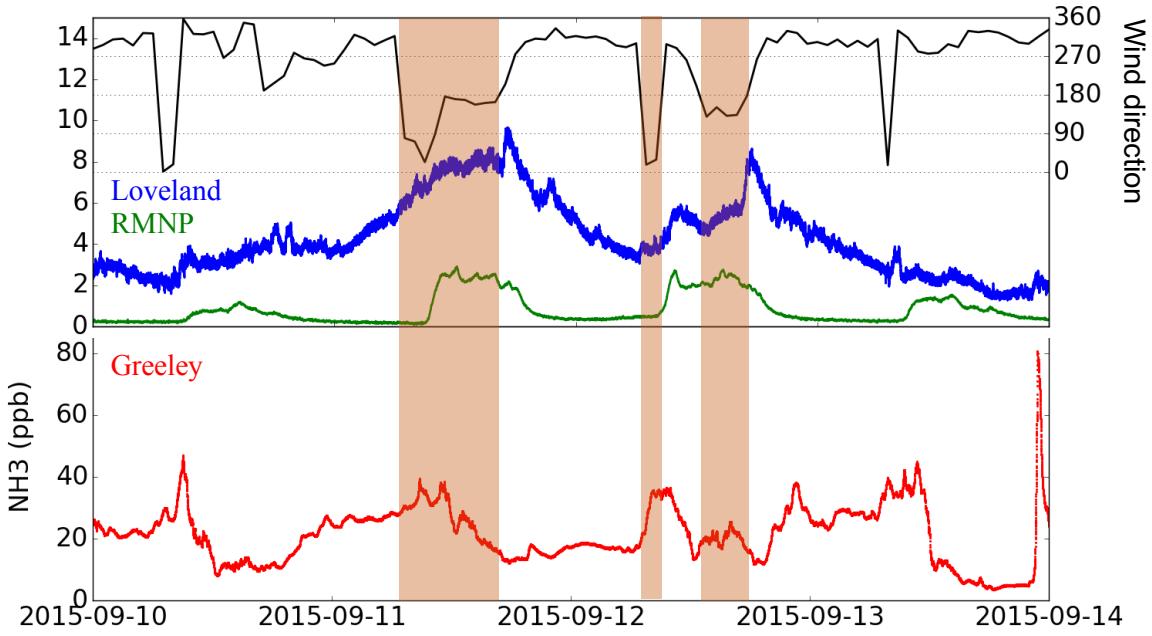

Figure 3.4.4 Measurements of ammonia concentrations in Greeley (red), Loveland (blue) and RMNP(green) from 09/10/2015 to 09/14/2015. Wind direction measured at the RMNP site is plotted in black. The shaded period indicates when upslope easterly flow occurs at RMNP.

To provide context to the upslope event that occurred on 09/11/15 at RMNP, NH_3 concentrations from 09/10/15 to 09/14/15 were plotted for all three observation sites. Over this period ammonia concentrations in Greeley varied greatly over the course of a day, ranging from 4.9 to 80.1 ppb, while the ranges of concentrations observed in Loveland and RMNP were 1.8 ppb – 10.1 ppb and 0.11 ppb – 2.4 ppb, respectively. For the whole period, it is shown that the

predominant wind direction in RMNP was from the west (180-360°). On 09/11/2015, a period of continuous upslope flow occurs with wind directions from 0-180° highlighted by the shaded area in Figure 3.4.4. Meanwhile, we see that the concentrations of ammonia measured in Loveland increase accordingly during this upslope period to 9.8 ppb, twice the maximum of the day before. In addition, the ammonia measured in RMNP on 09/11/2015 also peaked around 3.4 ppb, approximately 3 times of the maximum of the previous day. On the following day (09/12/2015), upslope easterly transport is also observed, and higher concentrations of ammonia were also measured at the Loveland and RMNP sites compared to observations on days without clear upslope flow. A few similar upslope cases were observed during the measurement period, accompanied by increased ammonia concentrations when there is no precipitation associated with the upslope transport. When precipitation occurs together with upslope transport flow, it has been found that the concentration of ammonia decreases rapidly due to wet scavenging and contributes to wet nitrogen deposition (Malm et al., 2009).

3.4.4 Transport of Ammonia Plume and On-Road Measurements

The above analysis and previous studies have shown that high levels of ammonia in the eastern plains of Colorado can be transported to RMNP and contribute to periods of high ammonia concentrations in the park (Malm et al., 2013). However, the spatial distribution of transported ammonia is not well described. It is possible that ammonia is transported as a set of distinct source plumes or it might be relatively homogeneous if the source plumes mix through dispersion prior to reaching the Rocky Mountains. Here we attempt to better quantify the distribution of ammonia at high time and spatial resolution and the associated transport pattern, using on-road measurement data acquired from the mobile platform made during June 2016. As

shown in figure 3.4.5, the mobile measurements of ammonia were plotted together with the HYSPLIT back-trajectory modeled results using same configuration described in Chapter 3.3. Instead of running HYSPLIT on each hour, a few NH_3 hotspots were selected and 6-hr back trajectories were run. The trajectories provide a rough idea of how ammonia was transported to the measurement location during the past 6 hours and the relative locations of CAFOs provide information of major ammonia emission sources. Here we see that instead of being spatially homogeneous, the transport of ammonia seems to be in distinct plumes. The back trajectory originated from the circled region near Timnath, where high levels of ammonia were observed, appears to have passed a large CAFO near Greeley. Between the CAFO and Timnath it appears that the trajectory also is associated with a region of elevated ammonia near Windsor. If one looks north and south of this Windsor crossing, one sees lower ammonia concentrations, suggesting that a distinct plume has been observed.

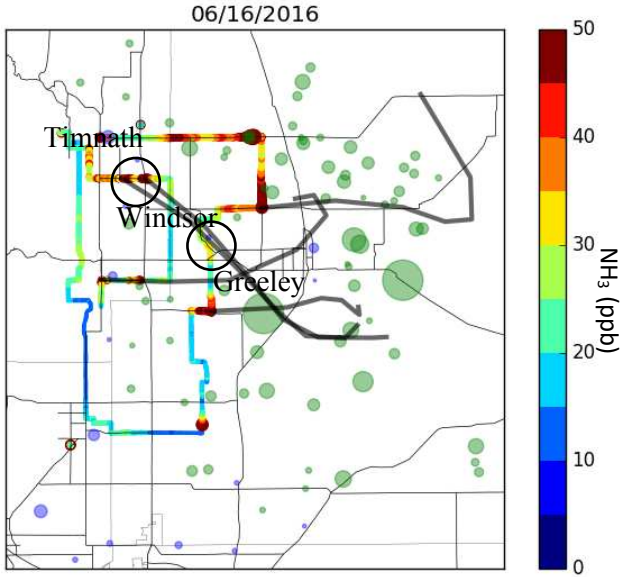

Figure 3.4.5 Mobile measurements of on-road ammonia on 16th June 2016. The colored line indicates driving routes and associated ammonia concentrations (ppb). Green dots indicate CAFOs scaled to maximum animal units allowed. Blue dots indicate waste water treatment plants (WWTP) scaled by designed flow (millions of gallons per day (MGD)). Black lines indicate HYSPLIT 6 hour back trajectory model results from selected NH_3 hotspots.

Unfortunately during the mobile measurement period there were no strong summer upslope events to investigate. Mobile measurements of N-S transects targeted in capturing easterly upslope transport of ammonia are of significant interest for future work. In addition, to further examine sources beyond animal feeding operations, such as waste water treatment plants and on-road vehicles, measurements of species other than ammonia, including methane and carbon monoxide should be included to use as tracers.

3.5 Evaluation of the Early Warning System

A pilot Early Warning System (EWS) has been in use in NE Colorado as a voluntary program with the agricultural community since April 2014. A small ensemble of forecasts using the Advanced Research and Forecasting (WRF-ARW) model is used for predicting the airflow from the eastern plains of Colorado to the Rocky Mountain National Park, and subsequent precipitation. The model is run routinely by the Precipitation Systems Research Group at Colorado State University and warnings are issued if large deposition period is forecasted for RMNP. Voluntary management practices are taken by agricultural producers to reduce potential emission of ammonia from agricultural sources.

Airflow from the ammonia source regions is predicted by calculating their trajectories in a 6-hour period. In this model, trajectories are released every 3 hours from Greeley, Fort Morgan and Limon, CO and integrated forward for 6 hours. Airflow that originated from Fort Morgan and Limon, CO rarely reach RMNP, so only air parcels released from Greeley are used for the model comparison with observations. In Figure 3.5.1 a map shows the distribution of trajectory release points and the distribution of CAFOs in Colorado. The trajectory-release points in Greeley nicely capture CAFOs within area, and are representative for agricultural-related

ammonia emission in Greeley. Model results were evaluated by comparing trajectories to ammonia concentrations measured in the park. Precipitation forecasts from the model were compared to the observed rainfall. In addition, warnings issued for potential large deposition events in RMNP were evaluated for its ability in predicting wet deposition amount and concentrations of N species within the wet deposition. Model results for the EWS used in this chapter are for 2015 period of when ammonia concentrations and wet deposition measurements in the RMNP site are available.

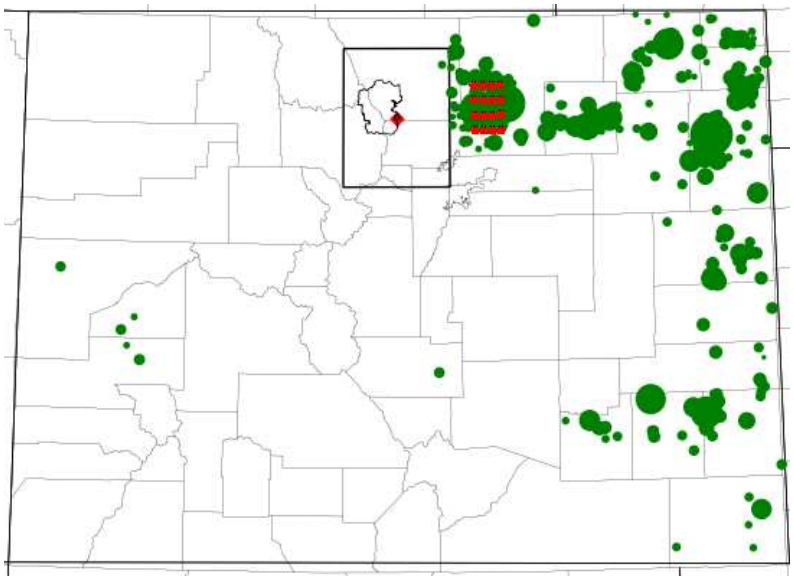

Figure 3.5.1. Map of trajectory releasing points and CAFOs. Red circles indicate trajectory releasing points; red diamond shows the RMNP site. RMNP is outlined, and animal units are plotted in green to indicate CAFOs. A 1°×1° box that centered in RMNP site is outlined.

To begin the evaluation of the model, a 1°×1° grid box was placed centered in the measurement site in RMNP, and the number of trajectory endpoints that fall in to the box was calculated daily. The percentage of the trajectory endpoints that falls close to the RMNP site (into 1°×1° grid box) was then obtained by dividing the total number of trajectories released from Greeley each day. The percentage of "close trajectories" is then compared to the daily

averaged ammonia concentrations measured by high time-resolution instrument with standard deviation shown. Collocated daily precipitation collected by a rain gauge in RMNP Long's Peak (ROM406) from the Clean Air Status and Trends Network (CASTNET) is available for the period of ammonia measurement (https://www3.epa.gov/castnet/site_pages/ROM406.html). The volume of fall precipitation was also determined from our bucket measurements of wet deposition when there was missing data for the precipitation amount measured by CASTNET.

Figure 3.5.2 shows time series plot of the ammonia concentrations, precipitation and percentage of model trajectories that fall within 1°×1° box above the measurement site. The percentage of the trajectories endpoints that fall within the box ranges between 0 to 45% during mid-June to mid-October 2015, and generally match the pattern of variation of ammonia concentrations during the period. The observed averaged daily concentrations of ammonia ranges from 0.5 to 3.3 ppb from mid-June to mid-October, with bigger daily variation associated with higher measured concentrations. However, large differences in patterns of ammonia level and endpoints percentage appear in the May 2015, especially for periods with high precipitation at the site, such as 05/03/15 - 05/09/15 and 05/11/15 - 05/16/15 when the model predicts high percentages of trajectory endpoints fall near the park while the concentrations of ammonia measure at the park stay low. This may be related to precipitation scavenging of pollutants along the way of transport, or local precipitation at the park that scavenges ammonia from the gas phase and deposits it as ammonium. In addition, it is shown (Figure 3.5.2) that in early spring 2015 the predicted trajectory endpoints rarely fall near the park with the maximum percentage of it below 20%, while the average daily concentrations of ammonia measured at the site range between 0.65-1.75 ppb, not being particularly low for the whole measuring period. This may indicate that sources of ammonia not related to the northeastern plains of Colorado are impacting

RMNP. Instead the relatively high levels of ammonia at the time may result from transport due to large scale meteorological system, or other local sources. An analysis of the large scale transport patterns during periods like this may be added in the future to the trajectory model to confirm impacts of large-scale transport on elevated ammonia concentrations in the RMNP.

Since ammonia can be removed from the gas phase to precipitation, only looking at the gas phase concentrations is not sufficient to provide a complete picture of the overall performance of the EWS in predicting local transport from the eastern plains to RMNP. The EWS was also designed to identify high wet deposition events which can only be evaluated using wet deposition data.

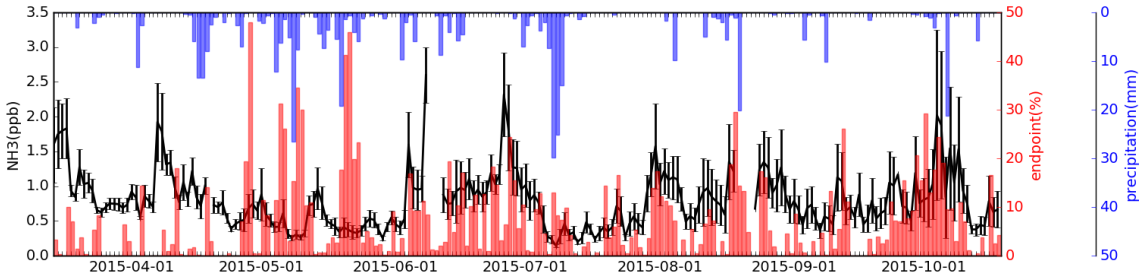

Figure 3.5.2 Comparison between ammonia concentrations (black lines), percentage of endpoints that fall into the 1°×1° box (red bars) and precipitation measurements from CASTNET (blue bars plotted downwards). Standard deviation of ammonia measurements for each day was also indicated.

In Figure 3.5.3 nitrogen deposition from March to October 2015 is plotted with the warning days highlighted. It is observed that a large fraction of wet nitrogen deposition in spring and early summer comes from organic nitrogen whereas more inorganic wet deposition is at late summer and fall. The higher fraction of organic nitrogen in total nitrogen wet deposition observed in spring and summer is expected due to higher biological activity (Jordon et al., 1995; Kieber et a., 2005; Drápelová, 2012). April to July are the most important months for high precipitation events and wet nitrogen deposition in 2015. This is consistent with the NADP

network data and past studies (Benedict et al., 2013a) showing that high nitrogen deposition occurs in spring and early summer at Loch Vale and Beaver Meadow sites in RMNP. Around 45% of the wet nitrogen deposition to the measuring site is in the form of ammonium, while 33% is in the form of nitrate. The warnings issued by the EWS in April capture the largest wet nitrogen deposition event in 2015 with total nitrogen deposition of 30 mgN/m^2 in 3 bucket-sampling days. Based on Figure 3.5.3, the warnings predict some of the largest wet nitrogen deposition events with precipitation amounts exceeding 10 mm, while failing to capture the daily precipitation events that occurred in May 2015. Continuous precipitation was observed in May 2015 while warnings were issued for some of the large precipitation events in the park with consideration of agricultural management practices that are not feasible for long-term implementation.

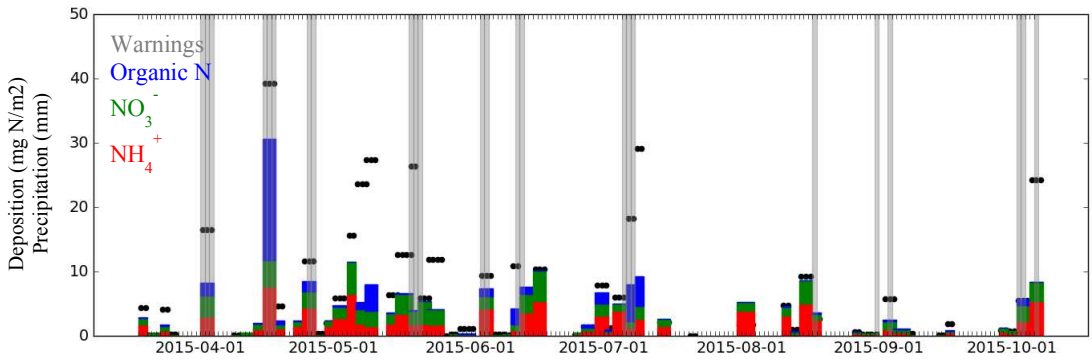

Figure 3.5.3 Stacked Nitrogen deposition (mg N/m^2) in 2015 with Organic Nitrogen deposition (blue), Nitrate deposition (green) and ammonium deposition (red). Black dots show precipitation amount (mm) measured by wet deposition bucket; Warning days is shaded (grey).

One of the project initiatives for the Early Warning System is to forecast for days with high potential of wet nitrogen deposition. Figure 3.5.4 shows the cumulative wet nitrogen deposition in 2015. The total cumulative wet deposition of nitrogen species in 2015 is 227.50 mg N/m^2 for the measuring period from mid-March to mid-October. Deposition events are marked

with a cross on top if they were forecasted and "warned". The 50th percentile and 75th percentile of the total wet nitrogen deposition is marked. Warnings were issued 12 times during the measuring period from March to October in 2015 with duration of 1 to 3 days. Most of the warnings fall above the 50th percentile of wet nitrogen deposition amount with one warning issued for wet nitrogen deposition amount that is below 50th percentile. For an ideal situation, the warnings issued by the Early Warning System would capture all large deposition events, such as ones above 75th percentile or a specific amount identified by stakeholders. The total wet nitrogen deposition that was forecasted by the EWS is 88.26 mg N/m^2, accounting for around 39% of the total wet nitrogen deposition amount for the entire bucket-measuring period from March to October.

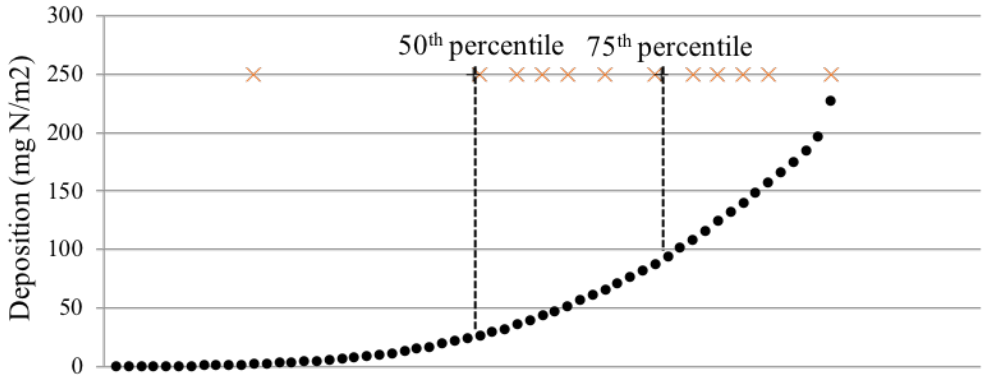

Figure 3.5.4 Cumulative wet nitrogen deposition (mg N/m^2) in 2015. Cumulative nitrogen deposition is indicated in black dots; red marks indicate deposition events that were forecasted and sent warnings for. The 50th and 75th percentile in is indicated for the cumulative total wet nitrogen deposition.

The Early Warning System in the Front Range shows skill in predicting transport of air flow from the source regions to the park, whereas ammonia concentrations in the measurement site in RMNP demonstrate more variability which might be impacted by precipitation along the transport path or local precipitation washout. Warnings issued by the Early Warning System

demonstrates ability in predicting the wet nitrogen deposition events that are above the 50th percentile, and needs to be improved for forecasting smaller precipitation in the park. Long-term measurements of wet nitrogen deposition and speciation should be carried for a more complete evaluation over a longer time period. The effectiveness of the voluntary efforts taken by agricultural producers should also be included in future investigation, to examine the ability of EWS in terms of reducing nitrogen deposition in the park.

CHAPTER 4 - SUMMARY AND CONCLUSIONS

Ammonia can be measured by several different techniques but there are few comparisons of these methods and potential biases exist in the methods. In this study we compared NH_3 measurements made by the Picarro CRDS and Air Sentry IMS and also the URG denuder/filter systems. The URG denuder/filter systems tended to measure lower ammonia concentrations than the measurements made by the high-time resolution instruments. Part of this difference appears to come from loss of ammonia in the nitric acid collection denuder situated upstream in the sample train. A positive bias in the continuous ammonia measurement methods might derive from interfering compounds (e.g., volatilized fine particle ammonium or amines). Operation of multiple co-located ammonia sampling instruments is advised as a routine check on method performance.

The NH_3 sampling techniques were applied to understand the spatial and temporal characteristics of atmospheric reactive nitrogen, especially ammonia in the regions of NE Colorado and RMNP during the spring to fall period. Continuous measurements of ammonia were also performed at three sites across the NE Colorado to help document the westward transport of ammonia from NE Colorado into RMNP and daily measurements of trace gases and chemical composition of particulate matter were made at RMNP. In addition to the high temporal measurements, a mobile platform was also deployed in June 2016 to examine the spatial variability of ammonia at high-time resolution.

Analyses of temporal variability of reactive nitrogen species were made on daily and seasonal time scales across the three sites. We observed different diurnal variabilities in ammonia at RMNP and Greeley with the continuous high-time resolution measurements. NH_3

concentration increases in the mid-to-late morning in RMNP are likely due to changes in transport patterns, although evaporation of morning dew has also been shown to yield an early morning ammonia concentration increase at sunrise. Ammonia levels tend to build up during the night in Greeley and decrease rapidly after sunrise as the boundary layer deepens. Seasonal variation of ammonia concentrations was consistent with previous studies showing higher ammonia concentrations measured in early summer to fall, and largely impacted by meteorological factors, especially precipitation and temperature.

Considerable variability in average ammonia concentrations existed in NE Colorado across the measurement sites. Much higher NH_3 concentrations were found close to confined animal feeding operations, and the real-time measurement at the Greeley site revealed much higher ammonia concentrations than the other two sites during the period of measurement. When combined with the HYSPIT model results, we observed from the mobile measurements, that spatial distribution of ammonia concentrations in the eastern plains of CO is largely impacted by meteorological factors, especially the prevailing wind. Elevated ammonia concentrations are usually found downwind of the agricultural source region with distinct plumes of ammonia being transported across the area over large distances. Analyses were made with wind roses and conditional probability revealing that transport from the eastern plains of CO contributes to elevation of ammonia concentrations in RMNP.

The performance of the Early Warning System predictions were evaluated with ammonia concentrations and measurements of wet deposition of nitrogen compounds. During the summer and early fall of 2015, the ratio of model trajectory endpoints that cross into the park region usually shows a similar pattern to variations of NH_3 concentrations in the park. Exceptions to this pattern appear when precipitation occurs in the air mass and NH_3 is scavenged into falling

rain or snow. This scavenging can occur within the park as well as in precipitating air masses upwind. To examine how well the EWS predicts high nitrogen deposition events in RMNP, the warnings issued were paired with deposition events in the park. The majority of the warnings were issued for nitrogen deposition events that were above the 50th percentile but fail in capturing some high deposition periods.

CHAPTER 5 - FUTURE WORK

This study provides important advances in adding observations of trace gases and chemistry of particulate matter in RMNP, as well as measurements of continuous ammonia with high time resolution, both in-situ and on a mobile platform. Precipitation was also analyzed for wet deposition of nitrogen compounds. Such measurements have been continuing for the years following 2015 and the analysis of the multi-year dataset will provide more information in inter-annual variability of reactive nitrogen gases/particles and wet nitrogen deposition in northeastern Colorado and long-term trends in reactive nitrogen concentrations and deposition in RMNP.

The mobile platform in this study was deployed in June 2016, and was not able to capture events of classic upslope easterly transport due to the (sponsor-designated) timing of the measurements. It would be helpful to study plume evolution up into the mountains during the classic spring or fall upslope transport periods. In addition, ammonia emissions from sources such as wastewater treatment plans and heavy-traffic highways remain uncertain. More targeted mobile measurements should be included for further examination of ammonia emission from sources other than CAFOs and to capture classic upslope events.

The Early Warning System has continued operation in the years following 2015 to present, and a longer period of records will help in providing more comprehensive evaluation in terms of the forecast ability of the EWS for large nitrogen deposition events. This program is currently voluntary for agricultural producers to participate in and there is incomplete characterization of how well these management strategies help in reducing nitrogen deposition. An examination of how well these management strategies work, with a focus on changes to

ammonia emissions for implementation of different best management practices will be important if this program keeps operating.

REFERENCES

Ashbaugh, L.L., Malm, W.C. and Sadeh, W.Z., 1985. A residence time probability analysis of sulfur concentrations at Grand Canyon National Park. Atmospheric Environment (1967), 19(8), 1263-1270.

Andreae, M.O. and Crutzen, P.J., 1997. Atmospheric aerosols: Biogeochemical sources and role in atmospheric chemistry. Science, 276(5315), pp.1052-1058.

Baron, J.S., Ojima, D.S., Holland, E.A. and Parton, W.J., 1994. Analysis of nitrogen saturation potential in Rocky Mountain tundra and forest: implications for aquatic systems. Biogeochemistry, 27(1), pp.61-82.

Baron, J.S., Rueth, H.M., Wolfe, A.M., Nydick, K.R., Allstott, E.J., Minear, J.T. and Moraska, B., 2000. Ecosystem responses to nitrogen deposition in the Colorado Front Range. Ecosystems, 3(4), pp.352-368.

Baron, J.S., 2006. Hindcasting nitrogen deposition to determine an ecological critical load. Ecological Applications, 16(2), pp.433-439.

Beem, K.B., Raja, S., Schwandner, F.M., Taylor, C., Lee, T., Sullivan, A.P., Carrico, C.M., McMeeking, G.R., Day, D., Levin, E., Hand, J., Kreidenweis, S.M., Schichtel, B., Malm, W.C., Collett Jr, J.L., 2010. Deposition of reactive nitrogen during the Rocky Mountain Airborne Nitrogen and Sulfur (RoMANS) study. Environmental Pollution 158, 862-872.

Benedict, K.B., Carrico, C.M., Kreidenweis, S.M., Schichtel, B., Malm, W.C. and Collett, J.L., 2013a. A seasonal nitrogen deposition budget for Rocky Mountain National Park. Ecological Applications, 23(5), pp.1156-1169.

Benedict, K.B., Chen, X., Sullivan, A.P., Li, Y., Day, D., Prenni, A.J., Levin, E., Kreidenweis, S.M., Malm, W.C., Schichtel, B.A., 2013b. Atmospheric concentrations and deposition of reactive nitrogen in Grand Teton National Park. Journal of Geophysical Research: Atmospheres 118, 11,875-811,887.

Benedict, K.B., Day, D., Schwandner, F.M., Kreidenweis, S.M., Schichtel, B., Malm, W.C., Collett Jr, J.L., 2013c. Observations of atmospheric reactive nitrogen species in Rocky Mountain National Park and across northern Colorado. Atmospheric Environment 64, 66-76.

Bowman, W.D., Murgel, J., Blett, T. and Porter, E., 2012. Nitrogen critical loads for alpine vegetation and soils in Rocky Mountain National Park. Journal of Environmental Management, 103, pp.165-171.

Burns, D.A., 2004. The effects of atmospheric nitrogen deposition in the Rocky Mountains of Colorado and southern Wyoming, USA—a critical review. Environmental Pollution, 127(2), pp.257-269.

Cape, J.N., Cornell, S.E., Jickells, T.D. and Nemitz, E., 2011. Organic nitrogen in the atmosphere—Where does it come from? A review of sources and methods. Atmospheric Research, 102(1), pp.30-48.

Carson, J.E., 1963. Analysis of soil and air temperatures by Fourier techniques. Journal of Geophysical Research, 68(8), pp.2217-2232.

Chameides, W.L., Fehsenfeld, F., Rodgers, M.O., Cardelino, C., Martinez, J., Parrish, D., Lonneman, W., Lawson, D.R., Rasmussen, R.A., Zimmerman, P. and Greenberg, J., 1992. Ozone precursor relationships in the ambient atmosphere. Journal of Geophysical Research: Atmospheres, 97(D5), pp.6037-6055.

Crutzen, P.J. and Lawrence, M.G., 2000. The impact of precipitation scavenging on the transport of trace gases: A 3-dimensional model sensitivity study. Journal of Atmospheric Chemistry, 37(1), pp.81-112.

Day, D.E., Chen, X., Gebhart, K.A., Carrico, C.M., Schwandner, F.M., Benedict, K.B., Schichtel, B.A. and Collett, J.L., 2012. Spatial and temporal variability of ammonia and other inorganic aerosol species. Atmospheric environment, 61, pp.490-498.

Drápelová, I., 2012. Organic and inorganic nitrogen in precipitation and in forest throughfall at the Bílý Kříž site (Beskydy Mts., Czech Republic). J For Sci, 58, pp.88-100.

Edgerton, E.S., Saylor, R.D., Hartsell, B.E., Jansen, J.J., Alan Hansen, D., 2007. Ammonia and ammonium measurements from the southeastern United States. Atmospheric Environment 41, 3339-3351

Eilerman, S.J., Peischl, J., Neuman, J.A., Ryerson, T.B., Aikin, K.C., Holloway, M.W., Zondlo, M.A., Golston, L.M., Pan, D., Floerchinger, C. and Herndon, S.C., 2016. Characterization of ammonia, methane, and nitrous oxide emissions from concentrated animal feeding operations in northeastern Colorado. Environmental Science & Technology.

Ellis, R.A., Murphy, J.G., Pattey, E., Haarlem, R.V., O'Brien, J.M. and Herndon, S.C., 2010. Characterizing a quantum cascade tunable infrared laser differential absorption spectrometer (QC-TILDAS) for measurements of atmospheric ammonia. Atmospheric Measurement Techniques, 3(2), 397-406.

EPA National Air Pollutant Emission Trends, 1900 - 1998 (https://hero.epa.gov/hero/index.cfm/reference/download/reference_id/12211)

Erisman, J.W., Galloway, J., Seitzinger, S., Bleeker, A. and Butterbach-Bahl, K., 2011. Reactive nitrogen in the environment and its effect on climate change. Current Opinion in Environmental Sustainability, 3(5), pp.281-290.

Fowler, D., Flechard, C., Skiba, U., Coyle, M. and Cape, J.N., 1998. The atmospheric budget of oxidized nitrogen and its role in ozone formation and deposition. The New Phytologist, 139(1), pp.11-23.

Galloway, J.N., Schlesinger, W.H., Levy, H., Michaels, A. and Schnoor, J.L., 1995. Nitrogen fixation: Anthropogenic enhancement-environmental response. Global Biogeochemical Cycles, 9(2), pp.235-252.

Galloway, J.N. and Cowling, E.B., 2002. Reactive nitrogen and the world: 200 years of change. AMBIO: A Journal of the Human Environment, 31(2), pp.64-71.

Galloway, J.N., Townsend, A.R., Erisman, J.W., Bekunda, M., Cai, Z., Freney, J.R., Martinelli, L.A., Seitzinger, S.P. and Sutton, M.A., 2008. Transformation of the nitrogen cycle: recent trends, questions, and potential solutions. Science, 320(5878), pp.889-892.

Garratt, J.R., 1994. The atmospheric boundary layer. Earth-Science Reviews, 37(1-2), pp.89-134.

Ge, X., Wexler, A.S. and Clegg, S.L., 2011. Atmospheric amines–Part I. A review. Atmospheric Environment, 45(3), pp.524-546.

Gebhart, K.A., Schichtel, B.A., Malm, W.C., Barna, M.G., Rodriguez, M.A. and Collett, J.L., 2011. Back-trajectory-based source apportionment of airborne sulfur and nitrogen concentrations at Rocky Mountain National Park, Colorado, USA. Atmospheric Environment, 45(3), 621-633.

Gebhart, K.A., Malm, W.C., Rodriguez, M.A., Barna, M.G., Schichtel, B.A., Benedict, K.B., Collett, J.L. and Carrico, C.M., 2014. Meteorological and back trajectory modeling for

the Rocky Mountain atmospheric nitrogen and sulfur study II. Advances in Meteorology, 2014.

Gruber, N. and Galloway, J.N., 2008. An Earth-system perspective of the global nitrogen cycle. Nature, 451(7176), pp.293-296.

Hegg, D.A., Radke, L.F., Hobbs, P.V. and Riggan, P.J., 1988. Ammonia emissions from biomass burning. Geophysical research letters, 15(4), pp.335-337.

Hill Jr, H.H., Siems, W.F. and St. Louis, R.H., 1990. Ion mobility spectrometry. Analytical Chemistry, 62(23), pp.1201A-1209A.

Hristov, A.N., Hanigan, M., Cole, A., Todd, R., McAllister, T.A., Ndegwa, P.M. and Rotz, A., 2011. Review: ammonia emissions from dairy farms and beef feedlots 1. Canadian journal of animal science, 91(1), pp.1-35.

Hutchinson, G.L., Mosier, A.R. and Andre, C.E., 1982. Ammonia and amine emissions from a large cattle feedlot. Journal of Environmental Quality, 11(2), pp.288-293.

Jordan, T.E., Correll, D.L., Weller, D.E. and Goff, N.M., 1995. Temporal variation in precipitation chemistry on the shore of the Chesapeake Bay. Water, Air, & Soil Pollution, 83(3), pp.263-284.

Kean, A.J., Harley, R.A., Littlejohn, D. and Kendall, G.R., 2000. On-road measurement of ammonia and other motor vehicle exhaust emissions. Environmental Science & Technology, 34(17), pp.3535-3539.

Kean, A.J., Littlejohn, D., Ban-Weiss, G.A., Harley, R.A., Kirchstetter, T.W. and Lunden, M.M., 2009. Trends in on-road vehicle emissions of ammonia. Atmospheric Environment, 43(8), pp.1565-1570.

Kieber, R.J., Long, M.S. and Willey, J.D., 2005. Factors influencing nitrogen speciation in coastal rainwater. Journal of Atmospheric Chemistry, 52(1), pp.81-99.

Kim, E. and Hopke, P.K., 2004. Source apportionment of fine particles in Washington, DC, utilizing temperature-resolved carbon fractions. Journal of the Air & Waste Management Association, 54(7), 773-785.

Lee, J.A. and Caporn, S.J.M., 1998. Ecological effects of atmospheric reactive nitrogen deposition on semi-natural terrestrial ecosystems. New Phytologist, 139(1), pp.127-134.

Lee, T., Yu, X.-Y., Ayres, B., Kreidenweis, S.M., Malm, W.C., Collett Jr, J.L., 2008a. Observations of fine and coarse particle nitrate at several rural locations in the United States. Atmospheric Environment 42, 2720-2732.

Lee, T., Yu, X.-Y., Kreidenweis, S.M., Malm, W.C., Collett, J.L., 2008b. Semi-continuous measurement of PM2.5 ionic composition at several rural locations in the United States. Atmospheric Environment 42, 6655-6669.

Li, Y., Schichtel, B.A., Walker, J.T., Schwede, D.B., Chen, X., Lehmann, C.M., Puchalski, M.A., Gay, D.A. and Collett, J.L., 2016. Increasing importance of deposition of reduced nitrogen in the United States. Proceedings of the National Academy of Sciences, p.201525736.

Malm, W.C., Collett J.L., Jr., Barna M.G., Gebhart K.A., Schichtel B.A., Beem K., Carrico C.M., Day D.E., Hand J.L., Kreidenweis S.M., Lee T., Levin E.J.T., McDade C.E., McMeeking G.R., Molenar J.V., Raja S., Rodriguez M.A., Schwandner F., Sullivan A.P., Taylor C., 2009. RoMANS: Rocky Mountain Atmospheric Nitrogen and Sulfur Study Report. ISSN 0737-5352-84, CIRA (Cooperative Institute for Research in the Atmosphere), Colorado State University, Fort Collins, Colorado.

Malm, W.C., Schichtel, B.A., Barna, M.G., Gebhart, K.A., Rodriguez, M.A., Collett Jr, J.L., Carrico, C.M., Benedict, K.B., Prenni, A.J. and Kreidenweis, S.M., 2013. Aerosol species concentrations and source apportionment of ammonia at Rocky Mountain National Park. Journal of the Air & Waste Management Association, 63(11), pp.1245-1263.

Matson, P., Lohse, K.A. and Hall, S.J., 2002. The globalization of nitrogen deposition: consequences for terrestrial ecosystems. AMBIO: A Journal of the Human Environment, 31(2), pp.113-119.

Miller, D.J., Sun, K., Tao, L., Pan, D., Zondlo, M.A., Nowak, J.B., Liu, Z., Diskin, G., Sachse, G., Beyersdorf, A. and Ferrare, R., 2015. Ammonia and methane dairy emission plumes in the San Joaquin Valley of California from individual feedlot to regional scales. Journal of Geophysical Research: Atmospheres, 120(18), pp.9718-9738.

Mizak, C.A., Campbell, S.W., Luther, M.E., Carnahan, R.P., Murphy, R.J. and Poor, N.D., 2005. Below-cloud ammonia scavenging in convective thunderstorms at a coastal research site in Tampa, FL, USA. Atmospheric Environment, 39(9), pp.1575-1584.

Mozurkewich, M., 1993. The dissociation constant of ammonium nitrate and its dependence on temperature, relative humidity and particle size. Atmospheric Environment. Part A. General Topics, 27(2), pp.261-270.

Pagans, E., Barrena, R., Font, X. and Sánchez, A., 2006. Ammonia emissions from the composting of different organic wastes. Dependency on process temperature. Chemosphere, 62(9), pp.1534-1542.

Paldus, B.A. and Kachanov, A.A., 2005. An historical overview of cavity-enhanced methods. Canadian Journal of Physics, 83(10), 975-999.

Park, R.J., Jacob, D.J., Field, B.D., Yantosca, R.M. and Chin, M., 2004. Natural and transboundary pollution influences on sulfate-nitrate-ammonium aerosols in the United States: Implications for policy. Journal of Geophysical Research: Atmospheres, 109(D15).

Phoenix, G.K., Hicks, W.K., Cinderby, S., Kuylenstierna, J.C., Stock, W.D., Dentener, F.J., Giller, K.E., Austin, A.T., Lefroy, R.D., Gimeno, B.S. and Ashmore, M.R., 2006. Atmospheric nitrogen deposition in world biodiversity hotspots: the need for a greater global perspective in assessing N deposition impacts. Global Change Biology, 12(3), pp.470-476.

Piña, A.J., 2017. A Social-Ecological Approach to Managing Agricultural Ammonia Emissions and Nitrogen Deposition in Rocky Mountain National Park (Doctoral dissertation, Colorado State University).

Pinder, R.W., Davidson, E.A., Goodale, C.L., Greaver, T.L., Herrick, J.D. and Liu, L., 2012. Climate change impacts of US reactive nitrogen. Proceedings of the National Academy of Sciences, 109(20), pp.7671-7675.

Potter, C., Klooster, S. and Krauter, C., 2003. Regional modeling of ammonia emissions from native soil sources in California. Earth Interactions, 7(11), pp.1-28.

Prenni, A.J., Levin, E.J.T., Benedict, K.B., Sullivan, A.P., Schurman, M.I., Gebhart, K.A., Day, D.E., Carrico, C.M., Malm, W.C., Schichtel, B.A. and Collett, J.L., 2014. Gas-phase reactive nitrogen near Grand Teton National Park: Impacts of transport, anthropogenic emissions, and biomass burning. Atmospheric Environment, 89, pp.749-756.

Puchalski, M.A., Sather, M.E., Walker, J.T., Lehmann, C.M., Gay, D.A., Mathew, J., Robarge, W.P., 2011. Passive ammonia monitoring in the United States: Comparing three different sampling devices. Journal of Environmental Monitoring 13, 3156-3167.

Rabalais, N.N., 2002. Nitrogen in aquatic ecosystems. AMBIO: A Journal of the Human Environment, 31(2), pp.102-112.

Ravishankara, A.R., Daniel, J.S. and Portmann, R.W., 2009. Nitrous oxide (N2O): the dominant ozone-depleting substance emitted in the 21st century. science, 326(5949), pp.123-125.

Sala, O.E., Chapin, F.S., Armesto, J.J., Berlow, E., Bloomfield, J., Dirzo, R., Huber-Sanwald, E., Huenneke, L.F., Jackson, R.B., Kinzig, A. and Leemans, R., 2000. Global biodiversity scenarios for the year 2100. science, 287(5459), pp.1770-1774.

Seinfeld, J.H., Pandis, S.N., 2012. Atmospheric chemistry and physics: from air pollution to climate change. John Wiley & Sons.

Shimshock, J.P. and Pena, R.G., 1989. Below-cloud scavenging of tropospheric ammonia. Tellus B, 41(3), pp.296-304.

Sobota, D.J., Compton, J.E. and Harrison, J.A., 2013. Reactive nitrogen inputs to US lands and waterways: how certain are we about sources and fluxes?. Frontiers in Ecology and the Environment, 11(2), pp.82-90.

Sommer, S.G. and Hutchings, N.J., 2001. Ammonia emission from field applied manure and its reduction—invited paper. European journal of agronomy, 15(1), pp.1-15.

Sommer, S.G., Schjoerring, J.K. and Denmead, O.T., 2004. Ammonia emission from mineral fertilizers and fertilized crops. Advances in agronomy, 82, pp.557-622.

Stelson, A.W. and Seinfeld, J.H., 1982. Relative humidity and temperature dependence of the ammonium nitrate dissociation constant. Atmospheric Environment (1967), 16(5), pp.983-992.

Stevens, C.J., Dise, N.B., Mountford, J.O. and Gowing, D.J., 2004. Impact of nitrogen deposition on the species richness of grasslands. Science, 303(5665), pp.1876-1879.

Sun, K., Tao, L., Miller, D.J., Khan, M.A. and Zondlo, M.A., 2014. On-road ammonia emissions characterized by mobile, open-path measurements. Environmental science & technology, 48(7), pp.3943-3950.

Sutton, M.A., Schjorring, J.K., Wyers, G.P., Duyzer, J.H., Ineson, P. and Powlson, D.S., 1995. Plant-atmosphere exchange of ammonia [and discussion]. Philosophical Transactions of the Royal Society of London A: Mathematical, Physical and Engineering Sciences, 351(1696), pp.261-278.

Sutton, M.A., Oenema, O., Erisman, J.W., Leip, A., van Grinsven, H. and Winiwarter, W., 2011. Too much of a good thing. Nature, 472(7342), pp.159-161.

Tao, L., Sun, K., Miller, D.J., Pan, D., Golston, L.M. and Zondlo, M.A., 2015. Low-power, open-path mobile sensing platform for high-resolution measurements of greenhouse gases and air pollutants. Applied Physics B, 119(1), pp.153-164.

Thompson, T.M., Rodriguez, M.A., Barna, M.G., Gebhart, K.A., Hand, J.L., Day, D.E., Malm, W.C., Benedict, K.B., Collett, J.L. and Schichtel, B.A., 2015. Rocky Mountain National Park reduced nitrogen source apportionment. Journal of Geophysical Research: Atmospheres, 120(9), pp.4370-4384.

Toth, J.J. and Johnson, R.H., 1985. Summer surface flow characteristics over northeast Colorado. Monthly weather review, 113(9), pp.1458-1469.

Townsend, A.R., Howarth, R.W., Bazzaz, F.A., Booth, M.S., Cleveland, C.C., Collinge, S.K., Dobson, A.P., Epstein, P.R., Holland, E.A., Keeney, D.R. and Mallin, M.A., 2003. Human health effects of a changing global nitrogen cycle. Frontiers in Ecology and the Environment, 1(5), pp.240-246.

Tsai, J.H., Lai, W.F. and Chiang, H.L., 2013. Characteristics of particulate constituents and gas precursors during the episode and non-episode periods. Journal of the Air & Waste Management Association, 63(1), 27-40.

Van Damme, M., Clarisse, L., Dammers, E., Liu, X., Nowak, J.B., Clerbaux, C., Flechard, C.R., Galy- Lacaux, C., Xu, W., Neuman, J.A. and Tang, Y.S., 2015. Towards validation of ammonia (NH 3) measurements from the IASI satellite. Atmospheric Measurement Techniques, 8(3), pp.1575-1591.

van den Berg, L.J., Jones, L., Sheppard, L.J., Smart, S.M., Bobbink, R., Dise, N.B. and Ashmore, M.R., 2016. Evidence for differential effects of reduced and oxidised nitrogen deposition on vegetation independent of nitrogen load. Environmental Pollution, 208, pp.890-897.

Vitousek, P.M., Aber, J.D., Howarth, R.W., Likens, G.E., Matson, P.A., Schindler, D.W., Schlesinger, W.H. and Tilman, D.G., 1997. Human alteration of the global nitrogen cycle: sources and consequences. Ecological applications, 7(3), pp.737-750.

von Bobrutzki, K., Braban, C. F., Famulari, D., Jones, S. K., Blackall, T., Smith, T. E. L., Blom, M., Coe, H., Gallagher, M., Ghalaieny, M., McGillen, M. R., Percival, C. J., Whitehead, J. D., Ellis, R., Murphy, J., Mohacsi, A., Pogany, A., Junninen, H., Rantanen, S., Sutton, M. A., and Nemitz, E.: Field inter-comparison of eleven atmospheric ammonia measurement techniques, Atmos. Meas. Tech., 3, 91–112, doi:10.5194/amt-3-91-2010, 2010.

Yu, X.-Y., Lee, T., Ayres, B., Kreidenweis, S.M., Malm, W. and Collett Jr, J.L., 2006. Loss of fine particle ammonium from denuded nylon filters. Atmospheric Environment 40, 4797-4807. Zbieranowski,

Wallace, J.M. and Hobbs, P.V., 2006. Atmospheric science: an introductory survey (Vol. 92). Academic press.

Wentworth, G.R., Murphy, J.G., Benedict, K.B., Bangs, E.J. and Collett Jr, J.L., 2016. The role of dew as a night-time reservoir and morning source for atmospheric ammonia. Atmospheric Chemistry and Physics, 16(11), pp.7435-7449.

Wheeler, M.D., Newman, S.M., Orr-Ewing, A.J. and Ashfold, M.N., 1998. Cavity ring-down spectroscopy. Journal of the Chemical Society, Faraday Transactions, 94(3), 337-351.

Wolfe, A.P., Baron, J.S. and Cornett, R.J., 2001. Anthropogenic nitrogen deposition induces rapid ecological changes in alpine lakes of the Colorado Front Range (USA). Journal of Paleolimnology, 25(1), pp.1-7.

Wolfe, A.H. and Patz, J.A., 2002. Reactive nitrogen and human health: acute and long-term implications. AMBIO: A Journal of the Human Environment, 31(2), pp.120-125.

Wolfe, A.P., Van Gorp, A.C. and Baron, J.S., 2003. Recent ecological and biogeochemical changes in alpine lakes of Rocky Mountain National Park (Colorado, USA): a response to anthropogenic nitrogen deposition. Geobiology, 1(2), pp.153-168.